Developmentally regulated alternate 3′ end cleavage of nascent transcripts controls dynamic changes in protein expression in an adult stem cell lineage

Cameron W. Berry,[1,11] Gonzalo H. Olivares,[1,2,3,4,5,6,7,8,9,11] Lorenzo Gallicchio,[1] Gokul Ramaswami,[10] Alvaro Glavic,[2,3,4] Patricio Olguín,[3,5,6,7] Jin Billy Li,[10] and Margaret T. Fuller[1,10]

[1]Department of Developmental Biology, Stanford University School of Medicine, Stanford, California 94305, USA; [2]Center for Genome Regulation (CRG), Universidad de Chile, Santiago 7810000, Chile; [3]*Drosophila* Ring in Developmental Adaptations to Nutritional Stress (DRiDANS), Universidad de Chile, Santiago 7810000, Chile; [4]Department of Biology, Faculty of Sciences, Universidad de Chile, Santiago 7810000, Chile; [5]Program of Human Genetics, Faculty of Medicine, Universidad de Chile, Santiago 8380453, Chile; [6]Department of Neuroscience, Faculty of Medicine, Universidad de Chile, Santiago 8380453, Chile; [7]Biomedical Neuroscience Institute (BNI), Faculty of Medicine, Universidad de Chile, Santiago 8380453, Chile; [8]Escuela de Kinesiología, Facultad de Medicina y Ciencias de la Salud, Universidad Mayor, Huechuraba 8580745, Chile; [9]Center of Integrative Biology (CIB), Universidad Mayor, Huechuraba 8580745, Chile; [10]Department of Genetics, Stanford University School of Medicine, Stanford, California 94305, USA

Alternative polyadenylation (APA) generates transcript isoforms that differ in the position of the 3′ cleavage site, resulting in the production of mRNA isoforms with different length 3′ UTRs. Although widespread, the role of APA in the biology of cells, tissues, and organisms has been controversial. We identified >500 *Drosophila* genes that express mRNA isoforms with a long 3′ UTR in proliferating spermatogonia but a short 3′ UTR in differentiating spermatocytes due to APA. We show that the stage-specific choice of the 3′ end cleavage site can be regulated by the arrangement of a canonical polyadenylation signal (PAS) near the distal cleavage site but a variant or no recognizable PAS near the proximal cleavage site. The emergence of transcripts with shorter 3′ UTRs in differentiating cells correlated with changes in expression of the encoded proteins, either from off in spermatogonia to on in spermatocytes or vice versa. Polysome gradient fractionation revealed >250 genes where the long 3′ UTR versus short 3′ UTR mRNA isoforms migrated differently, consistent with dramatic stage-specific changes in translation state. Thus, the developmentally regulated choice of an alternative site at which to make the 3′ end cut that terminates nascent transcripts can profoundly affect the suite of proteins expressed as cells advance through sequential steps in a differentiation lineage.

[*Keywords*: alternative polyadenylation; mRNA isoforms; translational control; spermatogenesis; mRNA isoforms]

Supplemental material is available for this article.

Received May 6, 2022; revised version accepted September 12, 2022.

The switch from proliferation to differentiation is a key event in both development and adult tissue renewal. Failure to cleanly shut down proliferation programs may contribute to the initiation of oncogenesis in the adult stem cell lineages that maintain short-lived differentiated cell populations and/or repair many tissues in the body. Conversely, delay or defects in turning on proper genetic programs for cell type-specific differentiation may lead to tissue dysmorphosis, degenerative disease, and aging.

Alternative mRNA processing resulting in cell type-specific mRNA isoforms may contribute to changes in cell state during differentiation (Ji et al. 2009; Di Giammartino et al. 2011; Lutz and Moreira 2011; Elkon et al. 2013; Gruber and Zavolan 2019; Cheng et al. 2020; Agarwal et al. 2021; Pereira-Castro and Moreira 2021; Sommerkamp et al. 2021). In particular, the selection of alternative sites at which to make the 3′ end cut that terminates the nascent transcript (termed alternative polyadenylation [APA]) leads to expression of mRNA isoforms with different 3′ UTR lengths (Di Giammartino et al. 2011; Shi 2012; Mueller et al. 2013). APA has been associated with specific cell types, disease states, and responses to extrinsic signals (Ji and Tian 2009; Ji et al. 2009; Mayr

[11]**These authors contributed equally to this work.**
Corresponding author: mtfuller@stanford.edu
Article published online ahead of print. Article and publication date are online at http://www.genesdev.org/cgi/doi/10.1101/gad.349689.122.

and Bartel 2009; Elkon et al. 2012; Morris et al. 2012; Gruber and Zavolan 2019; Mohanan et al. 2021). For example, developmentally regulated APA at many genes leads to expression of transcript isoforms with much longer 3′ UTRs in the brain than in other tissues (Ji et al. 2009; Hilgers et al. 2011; Derti et al. 2012; Smibert et al. 2012; Bae and Miura 2020), while oncogenic transformation has been correlated with the emergence of transcript isoforms with short 3′ UTRs due to APA (Mayr and Bartel 2009; Fu et al. 2011). Likewise, activation of T lymphocyte proliferation (by exposure to anti-CD3/CD28 beads) resulted in the expression of mRNAs with shorter 3′ UTRs due to APA (Sandberg et al. 2008).

Although changes in 3′ UTR length due to APA have been widely reported, including in *Drosophila* and mammalian testes (Smibert et al. 2012), the biological relevance of APA is poorly understood and has been extensively debated (Xu and Zhang 2020). While 3′ UTRs can harbor *cis*-regulatory information that controls translation of the mRNA, the extent to which widespread alternative 3′ end cleavage alters the proteome has been investigated in only a limited number of biological systems, for the most part in cell lines in vitro. For a small number of specific genes, transcript isoforms produced by alternative 3′ end cleavage were shown to be differentially translated in human cancer cell lines (Mayr and Bartel 2009). However, two global studies—one of translation in the mouse NIH3T3 cell line (Spies et al. 2013) and the other of protein abundance during the activation of murine T cells (Gruber et al. 2014)—both indicated that alternative 3′ end cleavage leading to different length 3′ UTRs had relatively little contribution to differential mRNA translation or protein abundance in the cell types assessed. On the other hand, a study of global translation in five human and two mouse cell lines found that transcript isoforms processed with short 3′ UTRs showed higher translational efficiency than those with long 3′ UTRs in all lines tested except for NIH3T3 cells (Fu et al. 2018). Likewise, analysis of ribosomal association of transcript isoforms in human HEK293T cells indicated that long 3′ UTR mRNA isoforms correlated with lower protein synthesis than short 3′ UTR isoforms from the same gene (Floor and Doudna 2016). While these recent studies indicate effects on mRNA translation in cultured cells, more than a decade after the identification of widespread APA, it has remained unclear whether biological systems use developmentally regulated alternative 3′ end cleavage as a mechanism to specify large-scale changes in protein expression in different cell types in vivo.

Here, using the *Drosophila* male germline as a model adult stem cell lineage (Fig. 1A), we show that developmentally regulated alternative 3′ end cleavage leading to production of transcript isoforms with shortened 3′ UTRs alters the translation state of many mRNAs in differentiating cells compared with their proliferating precursors. We found that >500 genes produce mRNA isoforms with long 3′ UTRs in proliferating spermatogonia but short 3′ UTRs soon after initiation of the program for meiosis and gamete differentiation in spermatocytes. Strikingly, differences in the behavior of mRNA isoforms

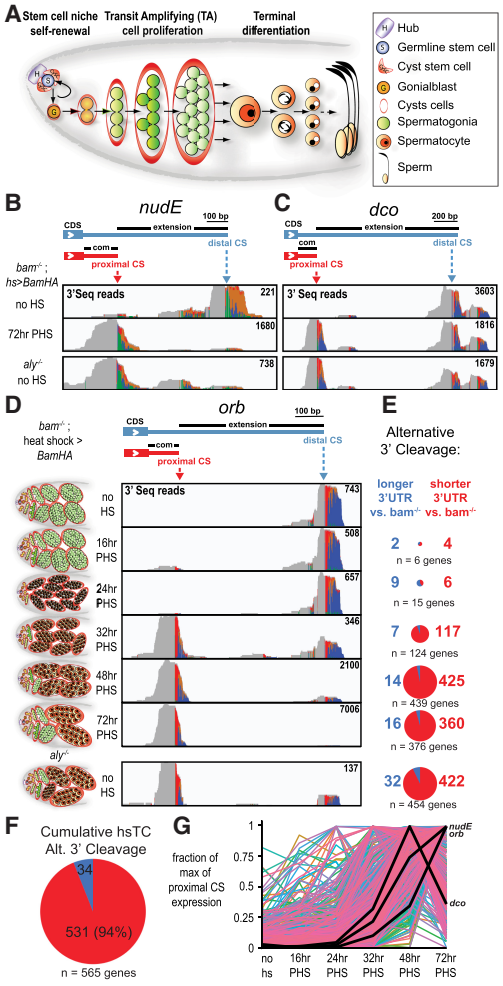

Figure 1. Differential 3′ end cleavage of selected transcripts is associated with the switch from spermatogonia proliferation to spermatocyte differentiation in *Drosophila*. (*A*) Main stages of *Drosophila* male germ cell differentiation. (*B*,*C*) 3′-seq tracks from one of two biological replicates plotted on the 3′ genomic region of *nudE* (*B*) and *dco* (*C*) from testes from $bam^{\Delta 86/1}$;*hs-Bam-HA* (*bam* heat shock time course [hsTC]) flies with no heat shock or 72 h post-heat shock (PHS), as well as testes from *aly* mutant flies with no heat shock. The maximum number of supporting reads is indicated at the *right* of each track. At the *top* is a gene model representing the two most abundant isoforms of 3′ UTR for each gene, indicating the position of the proximal (red) and distal (blue) cleavage sites (CSs) according to peaks from 3′-seq tracks. (*D*) 3′-seq tracks of one of two biological replicates plotted on the 3′ genomic region of *orb* from the *bam* hsTC flies at indicated times PHS and from *aly* mutant testes. At the *left*, testes diagrams indicate the cell diversity and developmental stage at each timepoint. (*E*) Pie charts (size normalized to gene list) for each time point indicating the number of genes detected as undergoing alternative 3′ cleavage events resulting in longer (blue) or shorter (red) 3′ UTRs relative to in testes from $bam^{\Delta 86/1}$;*hs-Bam-HA* flies without HS. (*Bottom* row) Comparison of $aly^{5p/2}$ flies without HS versus $bam^{\Delta 86/1}$;*hs-Bam-HA* flies without HS. (*F*) Cumulative pie chart containing all genes detected as changing 3′ UTR cut site in the *bam* hsTC. (*G*) Line graph of the 531 genes called as showing stage-specific alternative 3′ cleavage, with the relative level of the short 3′ UTR isoform plotted as the fraction of maximum value over the time course. (Black lines) Relative short 3′ UTR transcript levels for *nudE*, *orb*, and *dco*.

with short versus long 3′ UTRs in polysome fractionation studies suggested that for at least half of the genes, 3′ UTR shortening due to APA is accompanied by a change in translation state. For 50 genes, the long 3′ UTR isoform expressed in testes enriched for proliferating spermatogonia comigrated with subribosomal light fractions, suggesting the mRNA was not being translated, while the partner mRNA isoform with truncated 3′ UTR expressed from the same gene in testes enriched for differentiating spermatocytes comigrated with monosomes, disomes, or polysomes. For another 200 genes, transcript isoforms with a long 3′ UTR expressed in spermatogonia comigrated with monosomes, disomes, or polysomes, while their partner short 3′ UTR mRNA isoforms produced from the same gene in young spermatocytes migrated in lighter, subribosomal fractions, suggesting a lack of translation. For 139 of these 200 genes, the short 3′ UTR isoform moved from lighter, subribosomal fractions in extracts enriched for young spermatocytes to comigration with 80S or higher fractions in extracts enriched for maturing spermatocytes. This stage-specific on → off → on comigration of mRNA isoforms with ribosomes suggests a rationale for why the APA mechanism may be especially useful for dynamic regulation of protein production in a differentiation sequence: While 3′ UTR shortening by APA can specify a sharp decrease in protein production in early spermatocytes, transcription continues, providing mRNAs that can be translated at later stages, such as in maturing spermatocytes or spermatids undergoing morphogenesis. Our results suggest that developmentally regulated APA may provide a mechanism to facilitate clean and rapid transitions between developmental states via dynamic translational regulation, turning off the production of specific proteins for the prior program that may be deleterious for early steps of differentiation while maintaining transcripts and thus the ability to reactivate translation at later stages of differentiation.

Results

Stage-specific 3′ UTR shortening by APA in the Drosophila *male germline stem cell lineage*

Sperm are produced in large quantities throughout reproductive life in a robustly active adult stem cell lineage. The most dramatic changes in gene expression in this lineage occur when proliferating spermatogonia complete a final mitosis, undergo a last (premeiotic) S phase, and initiate the cell growth and differentiation program characteristic of spermatocytes. In *Drosophila* (Fig. 1A), male germline stem cells located at the apical tip of the testes normally divide one at a time, producing a replacement stem cell and a gonialblast, which becomes enclosed in a pair of somatic cyst cells and initiates spermatogonial proliferation. After four rounds of synchronous transit-amplifying mitotic divisions, the resulting 16 interconnected germ cells undergo premeiotic S phase in synchrony and then embark on the 3.5-d spermatocyte program, which takes place during meiotic prophase. The spermatocytes grow 25 times in volume and express many transcripts required for the meiotic divisions and the extensive cellular morphogenesis that takes place in the resulting haploid spermatids (Fuller 1993).

Wild-type testes contain a continuous stream of differentiating germ cells, each germline cyst at a different stage, making molecular analysis of stage-specific events challenging. However, germ cells can be induced to switch from proliferating spermatogonia to onset of spermatocyte differentiation in metasynchrony in vivo using a $bam^{-/-}$;*hs-Bam* time-course system (Kim et al. 2017). Briefly, in males mutant for *bag-of-marbles* (*bam*), testes fill with spermatogonial cysts in which the germ cells continue to proliferate and eventually die, never becoming spermatocytes. To induce semisynchronous differentiation of spermatogonia to spermatocytes in vivo, *bam* mutant flies carrying a heat shock-inducible transgene driving expression of Bam were subjected to a single 30-min pulse of heat shock at 37°C, returned to 25°C, and followed over time. Under this experimental setup, the spermatogonia complete their final mitoses and premeiotic DNA replication by 24 h post-heat shock (PHS), start to express markers of the early spermatocyte transcription program by 32 h PHS, and are filled with early, polar spermatocytes by 48 h PHS and with mid-stage maturing spermatocytes by 72 h PHS. The wave of differentiating germ cells enters the first meiotic division by 102 h PHS and ultimately differentiates into functional sperm by 12 d PHS (Kim et al. 2017). Note that because the $bam^{-/-}$;*hs-Bam* flies are returned to 25°C after the initial heat shock, $bam^{-/-}$ spermatogonia begin to accumulate again in the testes, so that testes from males 48 h PHS and even more so at 72 h PHS contain both differentiating spermatocytes and newly formed spermatogonia (see Fig. 1D, left diagrams).

To globally assess the changes in mRNA isoforms expressed due to APA as germ cells progress from spermatogonial proliferation to onset of the differentiation program in spermatocytes, we mapped the 3′ end cleavage sites of mRNAs expressed at different stages in male germ cell differentiation using 3′-seq, a modified version of RNA-seq that allows precise mapping of 3′ cut sites (Beck et al. 2010). Briefly, cDNAs representing short mRNA fragments including the polyA tail were sequenced in the sense direction, and transcript 3′ ends were identified by plotting sequence reads where the upstream part of the read matched a unique site in the genome but the downstream part contained multiple A residues not encoded in the genome (Fig. 1B–D). The analysis pipeline used to map 3′ cleavage sites required mapped reads to contain a stretch of at least 15 contiguous A residues with at least three not matching the genome (Materials and Methods; Supplemental Fig. S1A,B). To study alternative 3′ cleavage events that alter the length of 3′ UTRs rather than the protein-coding sequence, we focused on 3′-seq reads that mapped to 3′ UTR regions as defined by FlyBase version r6.36 plus up to 500 bp downstream (Supplemental Fig. S1J). Using these criteria, the number of 3′ end cleavage sites called per transcript was most often one (Supplemental Fig. S1K).

Comparing the 3′ ends of mRNAs expressed in testes from $bam^{-/-}$;*hs-Bam* flies before heat shock versus 48 or

72 h PHS revealed a set of ~500 genes that expressed mRNA isoforms with long 3′ UTRs at the 0-h time point, when the testes are filled with proliferating spermatogonia, but novel mRNA isoforms with shorter 3′ UTRs at 48 or 72 h PHS, when the testes have many early or mid-stage spermatocytes in addition to spermatogonia. For example, plotting the 3′-seq reads on genomic regions starting just before the stop codon and extending downstream for *nudE* (ortholog of mammalian NDEL1 [NudE neurodevelopment protein 1-like 1]) (Sasaki et al. 2000; Wainman et al. 2009) and *discs overgrown* (*dco*; ortholog of mammalian CKIε) (Fig. 1B,C; Jursnich et al. 1990; Kloss et al. 1998) revealed that the 3′ end cut site used in testes filled with spermatogonia mapped 615 nt (*nudE*) or 1557 nt (*dco*) downstream from the stop codon. In contrast, 3′-seq from testes 72 h PHS featured a new 3′ end cut and polyadenylation site much closer to the stop codon (121 nt for *nudE*; 122 nt for *dco*). Thus, the alternative 3′ UTR isoforms shared a short common region from the stop codon to the proximal cleavage site detected at 72 h PHS, but the main transcript expressed in 0-h $bam^{-/-}$; *hs-Bam* testes had a substantially longer 3′ UTR extending to a more distal cleavage site (Fig. 1B,C). The 3′ UTR shortening by APA was not due to the heat shock treatment, as similar short 3′ UTR mRNA isoforms were also observed in testes from flies that had not been subjected to heat shock but were mutant for the tMAC component *aly*, so the testes were filled with mature spermatocytes (Fig. 1B,C). For three selected genes tested, analysis by qRT-PCR of transcript isoforms expressed in mutant backgrounds that cause accumulation of spermatogonia or accumulation of arrested late spermatocytes validated the changes in 3′ UTR length during differentiation from spermatogonia to spermatocytes, as indicated by the 3′-seq results in the heat shock Bam time course (Supplemental Fig. S2A).

To determine whether most of the alternative polyadenylation (APA) events leading to expression of mRNA isoforms with shortened 3′ UTRs occurred at the same time in spermatocyte differentiation, we carried out 3′-seq analysis of testes from $bam^{-/-}$;*hs-Bam* flies at 16, 24, 32, 48, and 72 h PHS. Strikingly, for most genes subject to 3′ UTR APA, the switch to an alternative 3′ end cut site (i.e., proximal CS) occurred early in spermatocyte differentiation—in most cases by 48 h PHS, when the testes are filled with polar spermatocytes (Fig. 1D,E). Genome-wide 3′-seq analysis detected only six genes that had switched to an alternative 3′ end cut site by 16 h PHS and 15 genes that had switched by 24 h, based on our analysis criteria (Materials and Methods). However, comparing 3′-seq data from 32 h PHS, the time point at which many spermatocyte-specific mRNA markers were first detected, with $bam^{-/-}$;*hs-Bam* testes that were filled with proliferating spermatogonia because they had not been subjected to heat shock identified 124 genes that undergo alternative 3′ cleavage, with 117 (94.4%) producing transcripts with shorter 3′ UTRs at 32 h PHS (Fig. 1E). By 48 h PHS, when the testes were filled with young spermatocytes at the polar spermatocyte stage, a peak number of 439 genes showed APA, with 425 (96.8%) expressing mRNA isoforms with shorter 3′ UTRs at 48 h PHS than in the no heat shock starting condition (Fig. 1E). Seventy-two-hour PHS testes, which have abundant mid-stage apolar spermatocytes, showed APA at 376 genes (279 already detected at the 48-h time point) compared with the no heat shock starting condition. Cumulatively, over the initial 72 h of the time course, the genome-wide 3′-seq analysis identified 565 genes that produced mRNA isoforms with a difference in the position of the most abundant 3′ end cleavage site in the 3′ UTR in testes enriched for spermatocytes compared with in testes filled with proliferating spermatogonia but lacking spermatocytes (Fig. 1F). The time course analysis indicated that most of the APA events occurred at the young spermatocyte stage, with the vast majority (94%; 531 out of 565) resulting in the expression of mRNA isoforms with shorter 3′ UTRs as male germ cells differentiate (Fig. 1D–G). The 3′ UTR shortening due to APA observed in the time-course analysis was not a consequence of subjecting flies to heat shock, as similar shortened 3′ UTRs were observed in 3′-seq analysis of testes mutant for the spermatocyte-specific transcription regulator $aly^{-/-}$, which are filled with late stage spermatocytes (Fig. 1B–D, bottom rows). Likewise, analysis of single nuclear RNA-seq (snRNA-seq) data from testes produced by the Fly Cell Atlas Consortium (Li et al. 2022) confirmed 3′ UTR shortening in spermatocytes compared with spermatogonia for 90% (480 of the 531 genes) detected in our 3′-seq analysis of testes in the differentiation time course (Supplemental Fig. S3A–E).

Taken together, our global 3′-seq analysis of the differentiation time course and the 10X snRNA-seq results show that a selected set of genes produces mRNA isoforms with shortened 3′ UTRs due to utilization of an alternative, more proximal site at which to make the 3′ end cut on nascent transcripts after male germ cells undergo differentiation from spermatogonia into spermatocytes. For most genes exhibiting a switch in 3′ UTR length due to APA, the short 3′ UTR isoform reached its peak level by 48 h PHS, corresponding to early spermatocytes at the polar stage (Fig. 1G). At 72 h PHS, the relative detection of many of the spermatocyte-expressed shorter 3′ UTR isoforms decreased, perhaps in part due to the accumulation of new $bam^{-/-}$ spermatogonia in the $bam^{-/-}$;*hs-Bam* testes by 72 h PHS. For some genes subjected to APA, the level of the short 3′ UTR isoform continued to increase, possibly due to a substantial increase in levels of transcription from the locus by 72 h PHS. For example, for *orb* (Fig. 1D), which encodes an RNA-binding protein with well-known roles in oogenesis (Lantz et al. 1994), the first time point at which a significant number of alternative 3′ cleavage events leading to the production of the short 3′ UTR isoform (200 nt rather than the 1.2-kb 3′ UTR present at earlier time points) was detected was 32 h PHS. The level of expression and the ratio of short rather than long 3′ UTR *orb* mRNA isoforms increased at the later time points (48 and 72 h PHS). Again, similar short 3′ UTR transcripts predominated in testes from flies that had not been subjected to heat shock, where the testes were filled with arrested late spermatocytes due to loss of function of the meiotic arrest gene *aly* (Fig. 1D).

Cis-*regulatory elements differ at proximal vs. distal cleavage sites*

The set of genes subject to 3′ UTR shortening due to APA in early spermatocytes was enriched for weak polyadenylation signal (PAS) motifs (Retelska et al. 2006) near the proximal cut site paired with a strong or canonical PAS motif near the distal cut site. Over half (54.2%) of the 531 genes scored as producing mRNA isoforms with a long 3′ UTR in testes enriched for spermatogonia but a short 3′ UTR in testes enriched for spermatocytes had either a noncanonical or no known PAS just upstream of the main proximal cleavage site paired with a stronger or canonical PAS just upstream of the main distal cleavage site (Fig. 2A–C). De novo motif analysis by MEME of sequences extending from the distal cleavage site to 50 bp upstream for the genes that undergo alternative 3′ end cleavage identified the canonical PAS (AAUAAA) (Proudfoot and Brownlee 1976) as the most enriched (*e*-value 6.2×10^{-21}) motif relative to a background data set composed of 3′ cleavage sites of genes that did not undergo APA (Fig. 2A). As expected (Proudfoot and Brownlee 1976), the position of the PAS motif was ~28 nt upstream of the cleavage site. Mapping the AAUAAA motif to the genome (AATAAA; sense strand only) revealed that the canonical PAS was present within 50 nt upstream of the distal cleavage site in 65.7% of the genes that produce transcripts with long 3′ UTRs in *bam* mutant testes but short 3′ UTRs later in the time course (Fig. 2B). In contrast, only 22.8% of the genes identified as undergoing stage-specific APA in testes leading to mRNAs with shorter 3′ UTRs in spermatocytes had the canonical PAS sequence AATAAA within 50 nt upstream of the proximal cleavage site (Fig. 2B). In 80% of the APA genes, the proximal cut site instead had one of the 12 noncanonical (Retelska et al. 2006), weaker variants of the PAS just upstream (Supplemental Fig. S4A). Analysis of sequences downstream from the proximal and distal cleavage sites in both cases showed enrichment of the expected G/U-rich motif recognized by cleavage factor CstF64 (Supplemental Fig. S4B; MacDonald et al. 1994).

To test whether the pairing of weak proximal PAS with strong distal PAS was important for the stage-specific APA that results in the expression of mRNA isoforms with long 3′ UTRs in spermatogonia but short 3′ UTRs in spermatocytes, we constructed reporter transgenes containing the 3′ UTR region from *dco,* which shows 3′ UTR shortening by APA as male germ cells differentiate from spermatogonia to spermatocytes (Fig. 1C). Analysis of expression of a GFP-tagged *dco* fusion protein encoded by a large Fosmid-based transgene containing >23 kb of genomic DNA, including 5 kb upstream of and 10 kb downstream from *dco* (FlyFos TransgeneOme fTRG] project) (Sarov et al. 2016) showed that the Discs overgrown (Dco) protein was strongly expressed in the cytoplasm of germline stem cells (GSCs), gonialblasts (Gbs), and spermatogonia at the testis apical tip (Fig. 2D, solid bracket). However, expression of Dco-GFP from the Fosmid transgene was abruptly down-regulated when germ cells became spermatocytes (Fig. 2D, dotted bracket). The 3′ UTR region of the *dco* locus has a PAS variant (AATATA) upstream of the proximal cleavage site and a canonical PAS (AATAAA) upstream of the distal cleavage site. We constructed a matched pair of reporter transgenes for the *dco* locus, each of which contained the inducible UASt promoter (with 5× UAS repeats) upstream of the coding region for a destabilized GFP (Li et al. 1998) followed by genomic DNA encoding the entire long 3′ UTR sequence plus 500 bases of genomic DNA from the *dco* locus downstream from the distal cleavage site (Fig. 2E,F). In the wild-type reporter, the 3′ UTR contained the variant PAS AATATA 22 nt upstream of the proximal cleavage site and the canonical PAS AATAAA 33 nt upstream of the distal cleavage site, as in the endogenous *dco* locus (Fig. 2E). The mutated transgenic reporter *can-prox PAS** was identical except for a single nucleotide change that altered the variant proximal PAS AATATA to the canonical PAS AATAAA (Fig. 2F). The two transgenes were stably inserted into the same genomic attP landing site in separate *Drosophila* lines, and transcription of the reporters was induced specifically in germline stem cells and early spermatogonia using the *nanos-Gal4* expression driver to assess the effect of mutating the proximal PAS site on mRNA 3′ end processing in spermatogonia.

Analysis of expression of mRNA isoforms with long versus short 3′ UTRs in vivo from the two *dco* reporter transgenes transcribed in GSCs and early spermatogonia under control of *nos-Gal4* revealed that the single nucleotide change converting the variant PAS upstream of the proximal *dco* cleavage site to the canonical PAS was sufficient to allow 3′ UTR shortening in spermatogonia. Analysis by qRT-PCR to detect the ratio of mRNA from the GFP reporter transgene processed with the predicted long *dco* 3′ UTR relative to total GFP reporter mRNA revealed that for the reporter mutated to have the canonical PAS upstream of the proximal cleavage site (*can-prox PAS**), the ratio of the long 3′ UTR to total mRNA was 22-fold decreased relative to the wild-type reporter (Fig. 2G). The total level of mRNA expressed from the *can-prox PAS** reporter did not decrease relative to the wild-type reporter (Supplemental Fig. S4C). Together, these data suggest that, for the *dco* locus, an exact match to the canonical PAS AATAAA is required in spermatogonia for making the 3′ end cut that terminates nascent transcripts.

Imaging of GFP fluorescence in testes from flies carrying the reporters expressed under control of *nanos-Gal4* showed much lower levels of GFP in spermatogonia from the mutated transgene (Fig. 2J), which produced transcripts with the short 3′ UTR (Fig. 2G), even though the two reporters had the same protein-coding region sequence (Fig. 2E,F). Although the level of GFP fluorescence varied from cyst to cyst, as has been observed by others when the expression is driven under the control of Gal4/UAS (Skora and Spradling 2010), the reporter with the wild-type *dco* 3′ UTR showed substantial expression of GFP in proliferating germ cells at the tip of the testis (Fig. 2H), while the reporter mutated to contain a canonical PAS upstream of the proximal cleavage site (can-prox PAS*) resulted in a 20-fold decrease in GFP fluorescence,

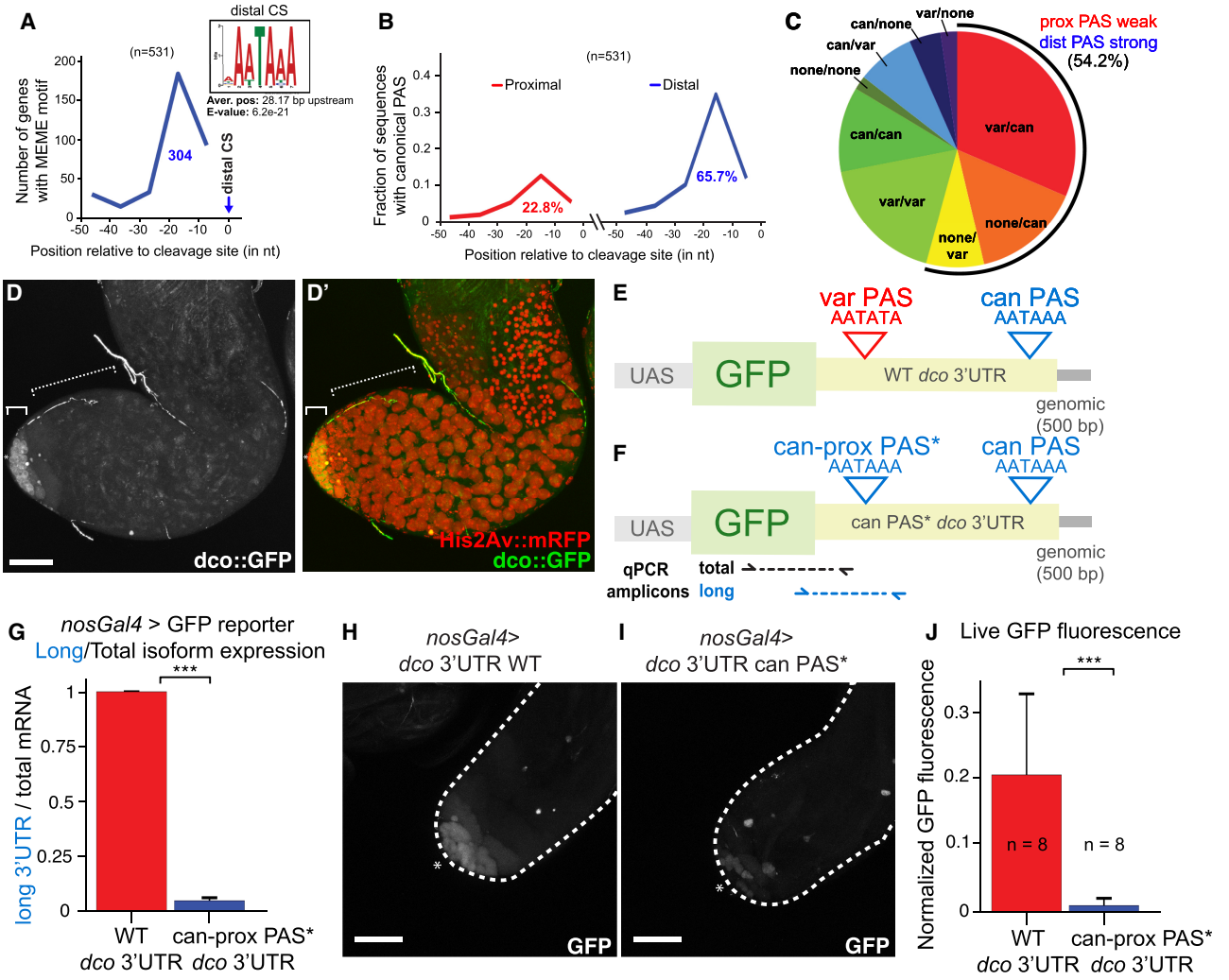

Figure 2. The strength of PAS at the proximal site influences stage-specific differential 3′ end formation. (*A*) Top MEME motif enriched in a 50-nt region upstream of distal cleavage sites (CSs) of 531 genes that undergo alternative 3′ cleavage to produce transcripts with shorter 3′ UTRs in later stages of the hsTC, compared with a background of similar 50-nt regions upstream of the 3′ end for genes that do not undergo alternative 3′ cleavage. Plot of the abundance of the MEME enriched sequence along the 50-nt region upstream of the distal CS, with the number of the APA transcripts that have the MEME motif 10–40 nt upstream of the distal cleavage site in blue. (*B*) Position of the canonical PAS (AATAAA) upstream of the proximal (red line) or distal (blue line) cleavage sites in genes identified as undergoing the stage-specific APA, with the percentage of the APA transcripts that have a canonical PAS 10–40 nt upstream of the respective cleavage sites shown. (*C*) Arrangement of canonical, variant, or no PAS motif upstream of the proximal and distal cleavage sites (indicated as "proximal/distal") in genes that undergo the stage-specific APA. (Black arc) Fifty-four percent of the APA genes have a stronger PAS associated with the distal cleavage site than with the proximal cleavage site. (*D*,*D*′) Live fluorescent images of testes from *Drosophila* containing a GFP-tagged third-copy Fosmid transgene for *dco* (green) and mRFP-tagged His2Av (red). (*E*,*F*) Diagram of the paired *dco* 3′ UTR reporter constructs. (Light gray) UAS element to drive cell type-specific expression in spermatogonia under the control of *nos-Gal4*, (light green) coding region for destabilized GFP, (light yellow) genomic DNA encoding *dco* 3′ UTR, (dark gray) 500 bases downstream from the distal 3′ cleavage site. (*E*) WT: Wild-type *dco* 3′ UTR with the proximal (variant sequence) and distal (canonical sequence) polyadenylation signal (PAS) indicated by a red and blue triangle, respectively. (*F*) can PAS* *dco* 3′ UTR: Same construct as above but with a single nucleotide change in the *dco* 3′ UTR that converts a variant PAS (AATATA) into the canonical PAS (AATAAA) 23 nt upstream of the proximal cleavage site. (*G*) RT-PCR ratio of reporter mRNA isoform with long 3′ UTR to total reporter mRNA produced in testes from the indicated reporters expressed in early germ cells under the control of *nos-Gal4* as measured by qRT-PCR using primer pairs indicated in *F*. WT *dco* 3′ UTR reporter long/total ratio was set to 1. Error bar indicates SD of at least three independent biological replicates. (*H*,*I*) Native GFP fluorescence for the respective reporters expressed at the apical tip of testes (indicated by an asterisk) under control of *nos-Gal4*. (*J*) Quantification of GFP fluorescence in z-stacks through apical tips of live testes, normalized to His2Av::mRFP expression. (Asterisk) Hub, (solid bracket) spermatogonia, (dashed bracket) spermatocytes. Scale bars, 50 µm. Statistical significance was determined by two-tailed Student's *t*-test. (***) *P*-value < 0.001.

with weak and variable expression detected in only a few germ cells at the testis tip (Fig. 2I,J). Together, these data suggest that (1) sequences in the long *dco* 3′ UTR expressed in spermatogonia may facilitate translation of the *dco* mRNA into protein, and (2) removal of these sequences in young spermatocytes by cleavage of nascent transcripts at the more proximal cut site may lead to an abrupt shutdown of Dco protein expression.

3′ UTR shortening by APA correlates with changes in protein expression

The changes in Dco protein expression as spermatogonia become spermatocytes led us to analyze the dynamics of protein expression in other cases of genes subject to 3′ UTR shortening due to APA where reagents to follow protein expression were available. Expression of the LolaF protein, encoded by mRNA isoforms resulting from 3′ UTR shortening due to stage-specific APA starting in young spermatocytes (Fig. 3A), showed regulatory dynamics reciprocal to the Dco protein. Immunostaining of wild-type testes with antibodies specific for the LolaF protein (Zhang et al. 2003) detected no signal in spermatogonia at the testis apical tip but abundant nuclear LolaF protein in spermatocytes (Fig. 3B). The timing of 3′ UTR shortening by APA correlated well with the onset of protein expression. Analysis by 3′ RACE of *lolaF* transcripts from testes at different stages of the heat shock time course confirmed that the change in the 3′ end cut site for *lolaF* occurred soon after the onset of spermatocyte differentiation, with the short 3′ UTR isoform appearing by 32 h PHS and persisting as the predominant 3′ RACE product through 48 h PHS (Fig. 3C). Strikingly, although the *lolaF* mRNA isoform with a long 3′ UTR was abundantly expressed in *bam* mutant testes based on our 3′-seq and 3′ RACE data (Fig. 3A,C), LolaF protein was not detected by immunostaining in $bam^{-/-}$;*hs-Bam* mutant testes either before heat shock or 16 h PHS (Fig. 3D,E). However, by 32 h PHS, correlating with the appearance of the short 3′ UTR mRNA isoform, LolaF protein detected by immunofluorescence staining was sharply up-regulated in the differentiating germ cells (Fig. 3F,G).

Analysis of expression of GFP-tagged fusion proteins encoded by large, Fosmid-based genomic transgenes available through the FlyFos TransgeneOme (fTRG) project showed several other cases of genes that encode mRNA isoforms with long 3′ UTRs in spermatogonia but short 3′ UTRs in spermatocytes where expression of the protein changed dynamically with male germ cell differentiation. Like Dco-GFP, the GFP-tagged fusion protein encoded by a Fosmid transgene for Chd3 was expressed in spermatogonia but not detected in young spermatocytes, correlating with 3′ UTR shortening by stage-specific APA (Fig. 3H,I). In contrast, the GFP-tagged fusion proteins encoded by Fosmid transgenes for the protein encoded by CG32006 (Fig. 3J,K) and the exonuclease Snipper (*Snp*) (Fig. 3L,M) were, like LolaF, up-regulated in spermatocytes compared with spermatogonia. In addition, immunofluorescence staining with antibodies against Numb (O'Connor-Giles and Skeath 2003) showed a lacework pattern of Numb protein localized at the periphery of spermatocytes but did not detect the protein in spermatogonia (Fig. 3N,O). The reciprocal dynamics of protein expression for the genes assessed suggest that a single molecular event, developmentally regulated APA, may trigger different changes in expression of the encoded proteins, with some going from off in spermatogonia to on in spermatocytes and others from on in spermatogonia to off in spermatocytes, presumably depending on the *cis*-regulatory sequences present in the different mRNA isoforms.

Polysome fractionation suggests 3′ UTR shortening correlates with switches in translation activity

To investigate globally whether changes in translation state may be a widespread consequence of stage-specific 3′ UTR shortening by developmentally regulated APA, we carried out polysome fractionation followed by 3′-seq. Lysates of testes from $bam^{-/-}$;*hs-Bam* flies 24 h PHS (enriched in transcripts with long 3′ UTRs), 48 h PHS (enriched in transcripts with short 3′ UTRs), or 72 h PHS were cleared of nuclei; layered on sucrose gradients; centrifuged to separate fractions with zero, few, or many ribosomes; and then assessed by 3′-seq to score comigration of mRNA isoforms (Fig. 4A,B; Supplemental Fig. S5A,B). The results revealed that shortening of the 3′ UTR by stage-specific cleavage of transcripts at the proximal site frequently correlated with dramatic differences in the position at which the two mRNA isoforms migrated in the polysome profiles. For 508 of the 531 genes that we identified as undergoing APA to produce mRNA isoforms with shorter 3′ UTRs as male germ cells differentiate from spermatogonia to spermatocytes, the depth of 3′-seq from the sucrose gradient fractions containing free RNA, 40S or 60S ribosomal subunits, 80S ribosomes, two to three ribosomes, or four or more ribosomes was sufficient to obtain information for how the long 3′ UTR mRNA isoform behaved in extracts from 24-h PHS testes and how the short 3′ UTR mRNA isoform behaved in extracts from the 48-h PHS testis samples. For one-quarter (124 out of 508) of the genes identified as undergoing stage-specific APA leading to 3′ UTR shortening with male germ cell differentiation, polysome fractionation suggested that the long 3′ UTR isoform expressed at early time points was translationally silent: The long 3′ UTR isoform was detected in the ribosome-free, 40S, and/or 60S ribosomal subunit-containing fractions but did not substantially comigrate with the fractions containing one, two to three, or four or more ribosomes in testis extracts from 24 h PHS (Fig. 4C). For 50 of these "long 3′ UTR off" genes, the short 3′ UTR isoform expressed from the same gene at 48 h PHS was detected in the fractions containing 80S monosomes, two to three ribosomes, or four or more ribosomes, indicating a substantial difference in the behavior of the mRNA isoforms (Fig. 4D).

For three-quarters (384 out of 508) of the genes identified as undergoing stage-specific APA leading to 3′ UTR shortening with male germ cell differentiation, the isoform with the long 3′ UTR expressed at 24 h PHS was detected in the fractions with one (80S), two to three, or four

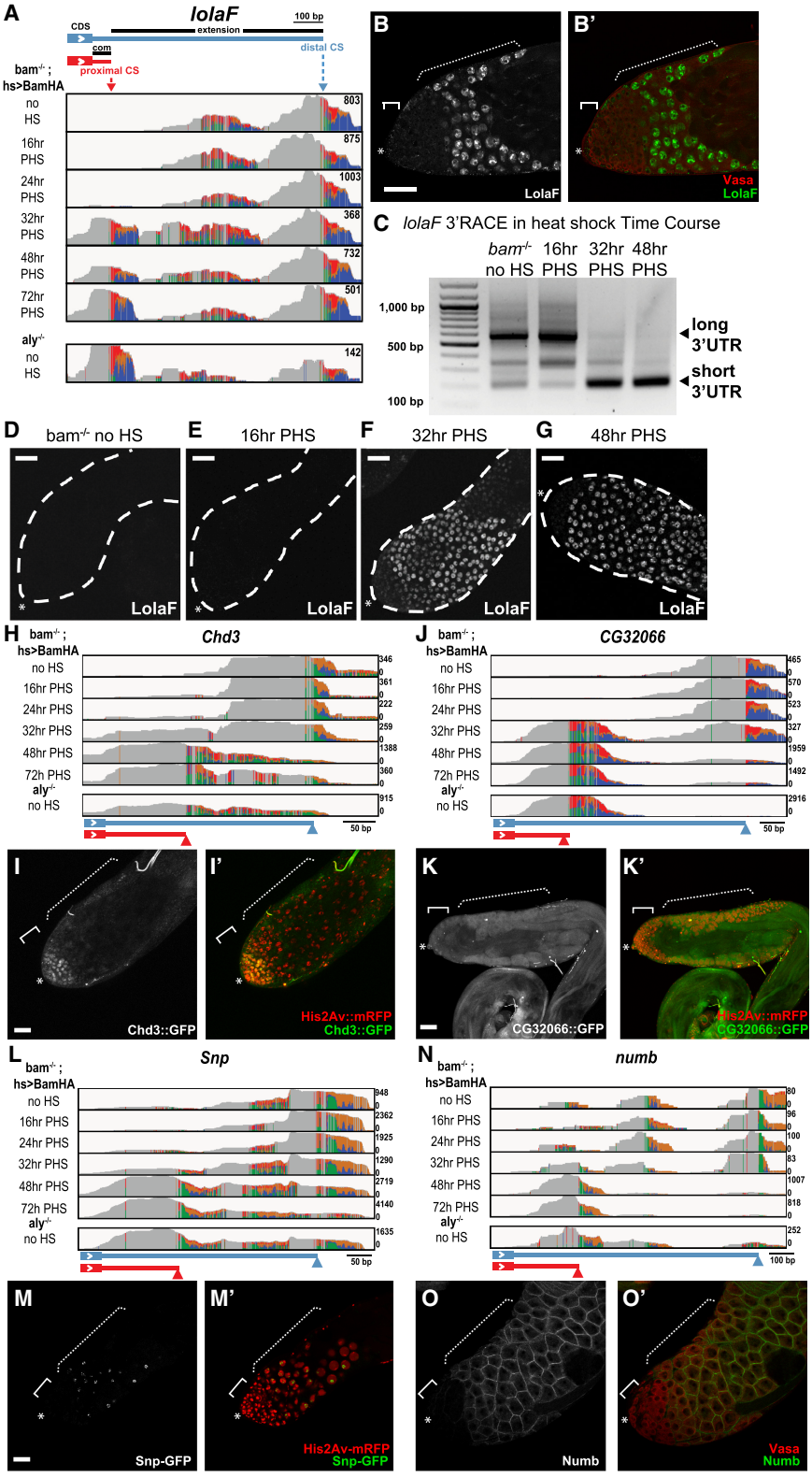

Figure 3. Changes in protein expression accompany the shortening of 3′ UTRs. (*A*) 3′-seq tracks of testis mRNA from one of two biological replicates plotted on the 3′ genomic region of *lolaF* from the *bam* hsTC at the indicated times PHS, as well as from and *aly* mutant testes. (*B*,*B*′) Immunofluorescence image of the apical region of a wild-type testis stained with anti-LolaF (white/green) and anti-Vasa (red) antibodies. (*C*) 3′ RACE of *lolaF* from *bam* hsTC fly testes at the indicated time points showing the expression of long and short 3′ UTR isoforms. (*D*–*G*) Immunofluorescence images containing the apical third of testes from $bam^{-/-}$;*hs-Bam* flies with no heat shock or 16, 32, or 48 h PHS stained with anti-LolaF antibody. (*H*,*I*,*L*,*N*) 3′-seq tracks from one of two biological replicates from testes from *bam* hsTC flies at the indicated times PHS, as well as from *aly* mutant testes, plotted on the 3′ genomic regions for *Chd3* (*H*), *CG32066* (*J*), *Snp* (*L*), and *numb* (*N*). (*Bottom*) Proximal (red arrowhead) and distal (blue arrowhead) cleavage sites were predicted from the most highly used cleavage site in $bam^{-/-}$;*hs-Bam* testes without heat shock and 48 h PHS, respectively. (*I*, *K*,*M*) Native fluorescence from GFP (white/green) and mRFP (red) in live-mount testes from flies carrying His2Av-mRFP and third-copy Fosmid-based GFP-tagged reporters for Chd3-GFP (*I*,*I*′), CG32066-GFP (*K*,*K*′), and Snp-GFP (*M*,*M*′). (*O*,*O*′) Immunofluorescence staining of testis tip with anti-Numb (white/green) and anti-Vasa (red). (Asterisk) Hub, (solid bracket) spermatogonia, (dashed bracket) spermatocytes. Scale bars, 50 µm.

or more ribosomes (Fig. 4E). Strikingly, for more than half (200 out of 384), the isoform with the short 3′ UTR expressed from the same gene was almost exclusively present in the free, 40S, and/or 60S fractions in testis extracts from 48 h PHS, indicating translational repression (Fig. 4F). Immunofluorescence staining of testes with available antibodies against the protein product of one of these genes, NudE (Wainman et al. 2009), revealed

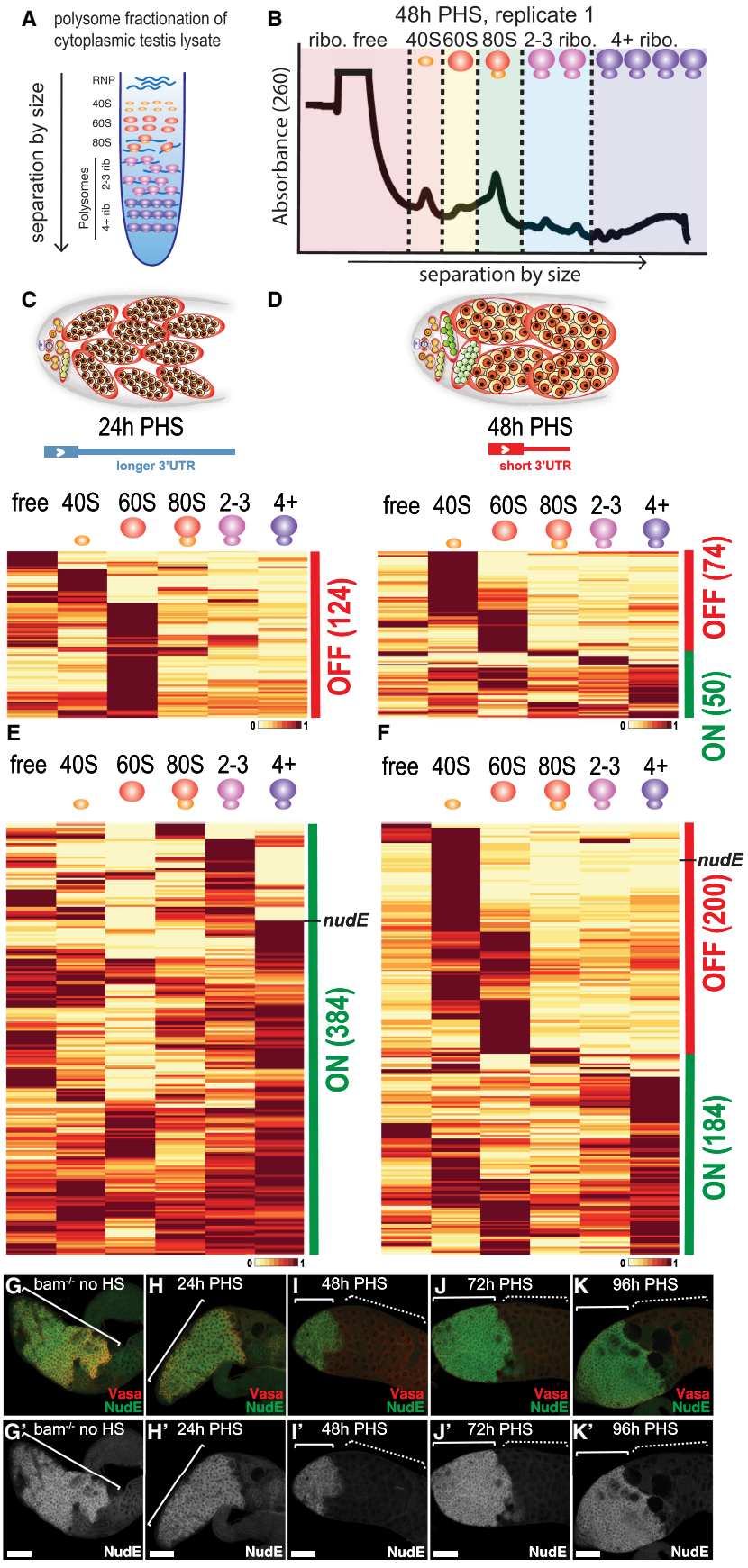

Figure 4. 3′-seq following polysome fractionation reveals widespread differences in migration of transcripts with long 3′ UTRs at 24 h PHS versus their short 3′ UTR isoforms at 48 h PHS. (*A*) Diagram of polysome fractionation by centrifugation: Transcripts occupied by more ribosomes sediment further down in the polysome profile. (*B*) Absorbance at 260 nm from one of two replicates of the polysome profile of testis extracts from 48 h PHS, indicating separation of the 40S, 80S, and multiple polysome peaks. ROYGBV colors (with dashed lines as boundaries) indicate the polysome fractions that were combined before 3′-seq. (*C*,*E*) 3′-seq from polysome profiling from 24-h PHS testes, plotting relative level of the long 3′ UTR isoform detected across the different polysome fractions (in each column) for genes that undergo the stage-specific 3′ UTR shortening due to APA (in each row). (*C*) Heat map of the 124 long 3′ UTR mRNA isoforms that predominantly comigrated with polysome fractions lighter than the 80S at the 24-h PHS time point. (*E*) Heat map of the 384 long 3′ UTR mRNA isoforms that comigrated with the 80S and/or polysomes at the 24-h PHS time point. (*D*,*F*) 3′-seq from polysome profiling of 48-h PHS testes, plotting relative level of the short 3′ UTR isoform detected across the different polysome profile fractions for genes that undergo the stage-specific 3′ UTR. (*D*) Heat map of distribution based on 3′-seq of the polysome fractions from 48-h PHS testes of the short 3′ UTR mRNA isoforms from the 124 genes grouped in *C*. (*F*) Heat map of distribution based on 3′-seq of the polysome fractions from 48-h PHS testes of the short 3′ UTR mRNA isoforms from the 384 genes from *E*. Heat map: White/yellow indicates low expression of the indicated transcript, and dark red indicates higher expression of the transcript. *nudE* transcript is indicated in black. (*G*–*K*′) Immunofluorescence images of testes from $bam^{\Delta 86/1}$;*hs-Bam* flies with no heat shock or 24, 48, 72, or 96 h PHS stained with anti-nudE antibody (white/green) and anti-Vasa (red). (Solid bracket) Spermatogonia, (dashed bracket) spermatocytes. Scale bars: 50 µm.

that the protein is strongly expressed in spermatogonia but is abruptly down-regulated in the young spermatocytes differentiating in testes 48 h PHS (Fig. 4G–I), as predicted from the migration behavior of the mRNA isoforms upon polysome fractionation (Fig. 4E,F; Supplemental Fig. S6A). Levels of immunofluorescence signal for NudE protein remained low in mid-stage spermatocytes present at 72 h PHS and the maturing spermatocytes present at 96 h PHS (Fig. 4J,K, dotted brackets), although high levels of immunofluorescence were detected in the $bam^{-/-}$ spermatogonia accumulating at the apical tip of the testes (Fig. 4J,K, solid brackets).

The results from polysome fractionation followed by 3′-seq suggest that the stage-specific switch in 3′ UTR processing that forms the 3′ end of nascent transcripts can result in dramatic changes in the interaction of the resulting mRNA isoforms with ribosomes. If this reflects changes in translation state, then developmentally regulated APA may allow sharp shifts in expression of many proteins as cells move from a proliferation program to onset of differentiation, with expression of some proteins switching from on to off and other proteins switching from off to on.

Reactivation of translation in later germ cell stages

Some mRNA isoforms with a short 3′ UTR due to APA that were translationally repressed at 48 h PHS began to comigrate with monosomes by 72 h PHS. For 199 of the 200 genes where the long 3′ UTR mRNA isoform migrated in fractions containing monosomes or higher numbers of ribosomes in 24-h PHS testis extracts while the short 3′ UTR isoform migrated in submonosomal fractions at 48 h PHS (Fig. 4E,F), there was sufficient read depth in fractions from polysome gradients of 72-h PHS testis samples to follow the migration behavior of the short 3′ UTR isoforms at the later time point (Supplemental Fig. S5C). For 69% of these 199 genes, the short 3′ UTR mRNA isoform showed significant enrichment in fractions comigrating with the 80S monosome (106 out of 199; 53%) and/or polysomes (33 out of 199; 16%) in lysates of testes taken 72 h PHS (Fig. 5A,B). For the remaining 31%, the short 3′ UTR mRNA isoform remained associated with submonosomal fractions at 72 h PHS, suggesting these transcripts remain translationally repressed.

cyclinB1 is an already known example of a gene that encodes an mRNA isoform with a long 3′ UTR that is translated in spermatogonia and a short 3′ UTR mRNA isoform that is translationally repressed in young spermatocytes but reactivated to produce protein in mature spermatocytes before the G2/M transition of meiosis I (White-Cooper et al. 1998; Baker et al. 2015). Consistent with this, the short 3′ UTR *cyclinB1* mRNA isoform expressed in spermatocytes migrated mostly in the 40S fraction in extracts from testes 48 h PHS but was substantially present in the 80S monosomal fraction by 72 h PHS (Fig. 5A,B; Supplemental Fig. S6B).

Antibody staining over the time course of spermatocyte maturation confirmed an additional example where polysome fractionation suggested that the short 3′ UTR mRNA isoforms were not translated in young spermatocytes but began to produce protein as spermatocytes mature. For *orb*, the long 3′ UTR mRNA isoform expressed in testes filled with proliferating spermatogonia (Fig. 1D, G) comigrated with polysomes in sucrose gradients of extracts of 24-h PHS testes (Fig. 5C, green line; Supplemental Fig. S5D). In contrast, the *orb* short 3′ UTR mRNA isoform expressed in testes filled with early spermatocytes (Fig. 1D,G) was detected predominantly in the 40S fraction in sucrose gradients from 48-h PHS testes (Fig. 5C, red line; Supplemental Fig. S5E). However, in extracts from 72-h PHS testes, the *orb* short 3′ UTR mRNA isoform showed a substantial increase in signal in the 80S monosome fraction (Fig. 5C, blue line; Supplemental Fig. S5F). Consistent with the behavior of *orb* mRNA isoforms in the polysome gradient fractionation assay, immunofluorescence staining with anti-Orb antibodies revealed Orb protein expressed in proliferating progenitor cells filling testes from $bam^{-/-}$;*hs-Bam* flies without heat shock or at 24 h PHS (Fig. 5D,E) but decreasing sharply in the early spermatocytes (marked by expression of Kumgang [Kmg]) (Kim et al. 2017) differentiating in testes 48 h PHS (Fig. 5F), consistent with the dramatic shift from comigration with polysomes at 24 h PHS to predominantly with the 40S fraction by 48 h PHS (Fig. 5C). However, consistent with the detection of some *orb* short 3′ UTR mRNA isoform in the 80S monosomal fraction by 72 h PHS (Fig. 5B,C) indicating possible reactivation of translation, testes from 96-h PHS flies showed an increase in immunofluorescence signal for Orb protein in late stage spermatocytes about to initiate the meiotic divisions (Fig. 5H, dotted bracket). Our results raise the possibility that 3′ UTR shortening due to stage-specific APA may allow many proteins robustly expressed in spermatogonia to be abruptly translationally silenced upon the switch to early spermatocyte stages while maintaining expression of a short 3′ UTR mRNA isoform that can be recruited to translation at later stages of germ cell differentiation (Fig. 6A–D).

Motifs enriched in 3′ UTR extensions of APA transcripts that change polysome profiles

Our results from polysome fractionation coupled with 3′-seq, antibody staining, and analysis of expression of GFP-tagged fusion proteins all indicate that stage-specific 3′ UTR shortening by developmentally regulated APA during differentiation in the male germline adult stem cell lineage is associated with widespread changes in protein expression. Strikingly, for some genes, the shift from long 3′ UTR to short 3′ UTR mRNA isoforms correlated with a switch from translation on in spermatogonia to off in early spermatocytes, while for other genes, the switch was from off in spermatogonia to on in spermatocytes. To explore whether the 3′ UTR extensions expressed in spermatogonia might be enriched for *cis*-acting sequences that either activate or repress translation of their mRNA isoform, we searched for sequence motifs enriched in two classes of 3′ UTR extensions. One class was the 200 APA genes where the long 3′ UTR isoform migrated with polysomes while the short 3′ UTR isoform migrated in ribosome-free fractions ("on to off") (Fig. 4F). The other class was the 50

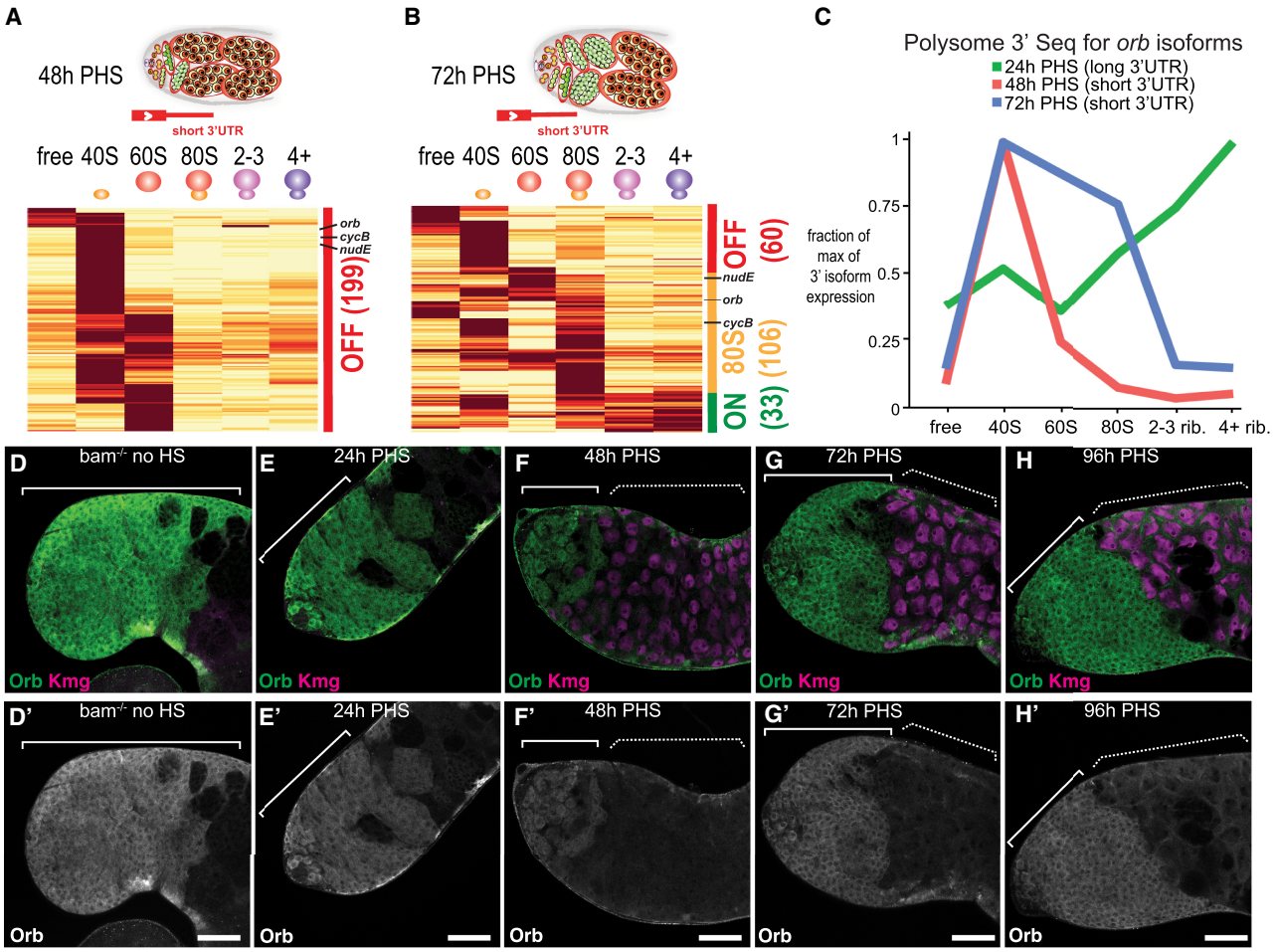

Figure 5. Dynamic changes in the polysome profile of short 3′ UTR isoforms as spermatocytes mature revealed by 3′-seq polysome profiling of 72-h PHS testes. (*A*) Heat map of distribution in the polysome gradient based on 3′-seq of 199 of the short 3′ UTR mRNA isoforms that predominantly comigrated with fractions lighter than the 80S monosome at the 48-h PHS time point from Figure 4F. (*B*) Heat map of distribution in the polysome fractions from 72-h PHS testes of the same 199 short 3′ UTR mRNA isoforms shown in *A*. (*C*) Line graph of relative levels of the long 3′ UTR *orb* isoform (24 h PHS; green) and short 3′ UTR *orb* isoform (48 h PHS [red] and 72 h PHS [blue]) in the indicated polysome fractions. (*D–H*′) Immunofluorescence images of apical regions of testes from $bam^{\Delta 86/1}$;*hs-Bam* flies with no heat shock or 24, 48, 72, or 96 h PHS stained with anti-Orb antibody (white/green) and antibody against the spermatocyte marker Kmg (magenta). (Solid bracket) Spermatogonia, (dashed bracket) spermatocytes. Scale bars, 50 µm.

APA genes where the long 3′ UTR isoform migrated in ribosome-free fractions while the short 3′ UTR isoform migrated with polysomal fractions ("off to on") (Fig. 4D).

De novo motif analysis using MEME of the "extension" region (sequence spanning from the proximal cleavage site used in spermatocytes to the distal cleavage site used in spermatogonia) of the 200 on-to-off APA transcripts revealed several motifs significantly enriched compared with a background data set of 3′ UTR sequences that are expressed in the germline but do not undergo APA (Fig. 6E). These included an [AU]-rich motif predicted to be bound by Shep, short polyA repeats predicted to be bound by PAbp, short polyU repeats predicted to be bound by Elav, and an [AC]-rich motif predicted to be bound by Cnot4 (Fig. 6E). Transcripts for all four of these RNA binding proteins were detected as expressed in spermatogonia in the single nuclear RNA-seq analysis carried out by the Fly Cell Atlas Consortium (Supplemental Fig. S8A–C,F; Li et al. 2022). De novo motif analysis using MEME of the "extension" region of the 50 off-to-on APA transcripts also revealed enrichment of an [AU]-rich motif, short polyU repeats, and an [AC]-rich motif (Fig. 6F). Thus, both classes of transcripts were enriched for motifs predicted to bind Shep, Elav, and Cnot4 in the long 3′ UTR isoform expressed in spermatogonia. The polyA motif, however, was enriched in the 3′ UTR extensions of the on-to-off but not the off-to-on transcripts. A tempting speculation is that recruitment of PAbp to polyA motifs in the long 3′ UTRs of on-to-off genes may facilitate mRNA translation in spermatogonia, with removal of the 3′ UTR extension in spermatocytes by APA abruptly shutting off translation. In addition, analysis of miRNA seed sequences in extension regions using simple enrichment analysis (SEA; MEME suite) of the off-to-on

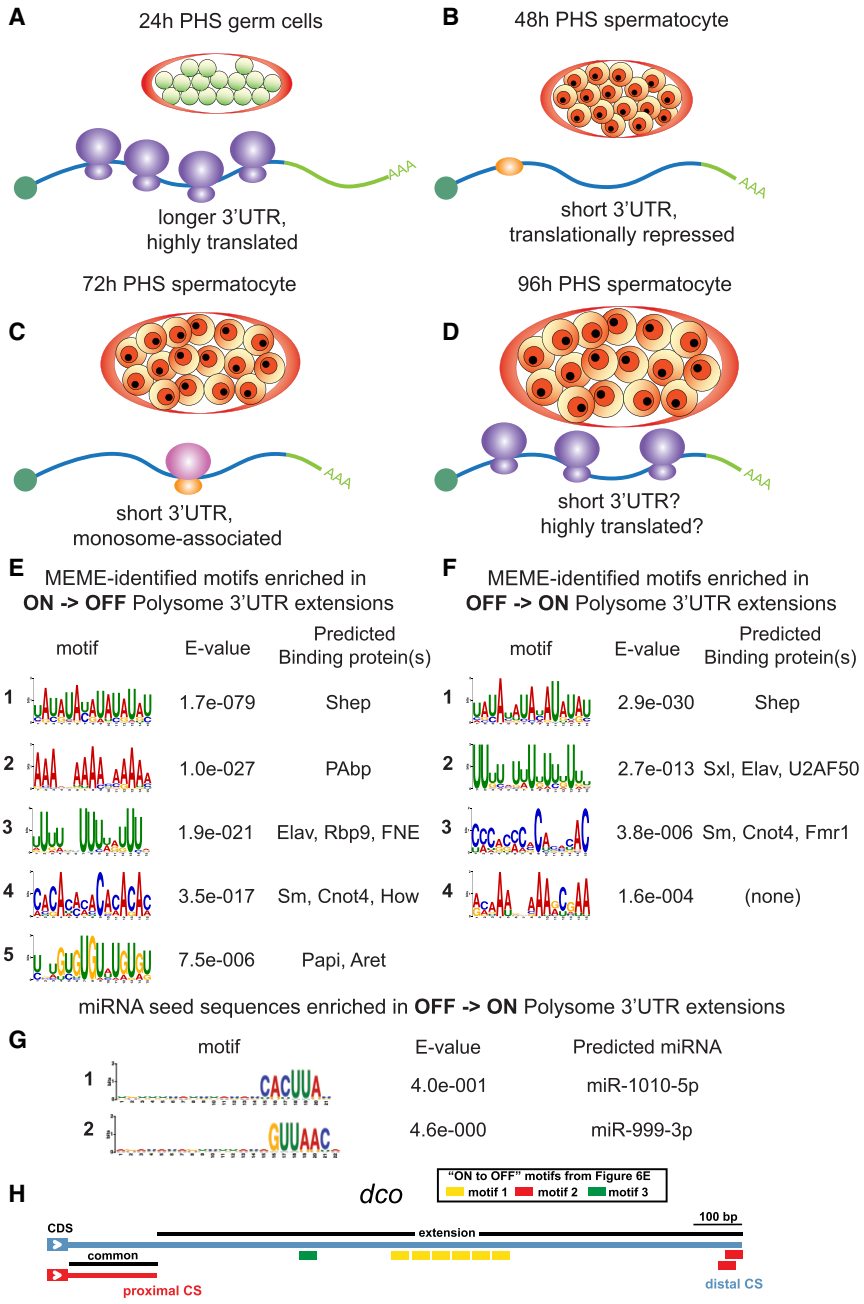

Figure 6. Identification of motifs enriched in transcripts from genes subject to APA that undergo dynamic translational regulation as *Drosophila* germline progenitors differentiate. Cartoon depictions of germline cysts from 24-h (*A*), 48-h (*B*), 72-h (*C*), and 96-h (*D*) PHS testes. Predicted transcript association with ribosomes based on 3′-seq polysome profiling with the coding region (blue) and 3′ UTR (green). Top MEME motifs enriched in the "extension" regions spanning from the proximal to distal cleavage sites of 200 transcripts that undergo APA and transition from on polysomes at 24 h PHS to polysome-free fractions at 48 h PHS (*E*) and 50 transcripts that undergo APA and transition from polysome-free fractions at 24 h PHS to polysomes at 48 h PHS (*F*). Predicted RNA binding proteins that bind to each motif are also indicated. (*G*) Indicated miRNAs are enriched in the 3′ UTR extensions of transcripts that go from off to on relative to a background set of 3′ UTRs that do not undergo APA. (*H*) The presence of motifs identified in *E* is indicated in the extension region of dco's 3′ UTR.

transcripts identified miR-1010-5p and miR-999-3p as the top two enriched miRNA seed sequences (Fig. 6G).

We note that for the 3′ UTR of *dco*, GFP protein was expressed in spermatogonia from a reporter transgene with GFP attached to the *dco* long 3′ UTR (Fig. 2E,H). However, when the *dco* 3′ UTR was cut short, expression of GFP in spermatogonia decreased 20-fold (Fig. 2F,I,J), suggesting that the *dco* long 3′ UTR extension contains sequences that increase translation of the mRNA in vivo. Strikingly, the *dco* 3′ UTR extension features six to seven overlapping AU-rich motifs (in a 66-nt-long string of AUAUAUAU), a polyU motif, and two overlapping polyA motifs (Fig. 6H).

Discussion

Here we show that a stage-specific change in 3′ end cleavage site choice leading to the production of mRNA isoforms with short rather than long 3′ UTRs can trigger dramatic and widespread changes in the suite of proteins expressed as cells progress from one developmental stage to the next in a differentiation lineage in vivo. In some cases, 3′ UTR shortening by developmentally regulated APA correlates with a switch from protein expression in proliferating spermatogonia to repression of translation in young, differentiating spermatocytes (on to off), while for other genes the switch is from no protein expressed

in spermatogonia to protein accumulation in spermatocytes (off to on). Thus, a single molecular event—developmentally regulated APA—can trigger changes in the expression of many proteins, likely depending on the *cis*-regulatory sequences present in the long 3′ UTR isoform expressed by individual genes.

Strikingly, the vast majority of APA events that we detected comparing testes filled with spermatogonia versus testes filled with spermatocytes resulted in expression of mRNA isoforms with much shorter 3′ UTRs in differentiating spermatocytes than the mRNA isoforms expressed from the same gene in the proliferating spermatogonial precursor cells. This is counter to the widespread observations of mRNA isoforms with shorter 3′ UTRs due to APA in proliferating cells; for example, after T cell activation or in cancer cells (Sandberg et al. 2008; Mayr and Bartel 2009). Thus, the 3′ UTR shortening observed upon T cell activation may not be a result of the demands of rapid cell proliferation, but rather a developmentally programmed event leading to consequences that affect cell state. In the case of cancer, the widespread expression of mRNA isoforms with short 3′ UTRs due to APA may contribute to cancer progression by allowing abnormal expression of oncogenic proteins usually translationally repressed via sequences in the longer 3′ UTRs expressed in normal cells (Sandberg et al. 2008; Mayr and Bartel 2009; Masamha et al. 2014; Xia et al. 2014). Thus, the mechanisms that normally ensure proper 3′ cut site selection in many mammalian cell types may be antioncogenic, much as is the proper function of genes involved in DNA repair such as BRCA1 and BRCA2, with defects that result in abnormal use of more proximal, less favored PASs selected for in tumor cells because they allow promiscuous expression of oncogenic proteins.

In another intriguing difference between our results and the classic studies of 3′ UTR shortening due to APA upon T cell activation, Sandberg et al. (2008) found that 3′ UTR shortening usually led to higher levels of protein expression than from similar constructs containing the long version of the 3′ UTR, an effect they surmised might be due to removal of miRNA target sites in the 3′ UTR extension. Although consistent with such a mechanism, we identified a number of cases where 3′ UTR shortening correlated with a switch in translation from off in spermatogonia (long 3′ UTR) to on in spermatocytes (short 3′ UTR), but substantially more of the cases we documented indicated the opposite: protein expression switching from on in spermatogonia to off in spermatocytes.

Our findings in the *Drosophila* male germline adult stem cell lineage may have implications for other cases where widespread, developmentally regulated APA has been well documented. In the nervous system, many genes express mRNA isoforms with long 3′ UTRs due to the use of a more distal PAS in differentiated cells (Tian et al. 2005; Zhang et al. 2005; Ji et al. 2009; Hilgers et al. 2011; Smibert et al. 2012; Ulitsky et al. 2012; Lianoglou et al. 2013; Miura et al. 2013; Bae and Miura 2020). The long 3′ UTRs may carry sequences important for cell type-specific subcellular localization or context-dependent translation of specific mRNAs in neurons. APA has been shown to play an essential role in the dendritic and axonal localization of several transcripts, with consequences on their local translation (Shigeoka et al. 2016; Taliaferro et al. 2016; Tushev et al. 2018; Andreassi et al. 2019), including brain-derived neurotrophic factor (BDNF) (An et al. 2008; Vicario et al. 2015), mTOR (Terenzio et al. 2018), and Shank (Epstein et al. 2014). In other cases, the extralong 3′ UTRs have been implicated in differential translational activity. For example, in rat hippocampal neurons, *glutamate receptor 2* (*GluR2*) transcript isoforms with short 3′ UTRs were enriched in polysome fractions, suggesting active translation, while *GluR2* transcript isoforms with long 3′ UTRs were preferentially enriched in ribosome-free sucrose gradient fractions, indicating translational silence. Interestingly, upon seizure induction, the long 3′ UTR mRNA isoforms shifted to polysome fractions, indicating a switch from translationally dormant to an actively translated state (Irier et al. 2009). Similarly, in dopaminergic neurons, dysregulation of an extended 3′ UTR mRNA isoform expressed from the α-*synuclein* (α-*SYN*) gene may contribute to Parkinson's disease. α-SYN protein is the major component of Lewy bodies associated with Parkinson's disease (PD) pathogenesis (Spillantini et al. 1997). The long 3′ UTR mRNA isoform of α-*SYN* has reduced translation compared with shorter 3′ UTR isoforms. However, this long 3′ UTR isoform was poorly represented in iPSC-derived dopaminergic neurons from sporadic PD patients (Je et al. 2018), suggesting a possible cause of pathological overexpression of α-SYN protein. In a counterexample, the *serotonin transporter* (*SERT*) gene encodes mRNA isoforms with a long 3′ UTR extension that contains a binding site for heterogeneous nuclear ribonucleoprotein K (hnRNPK), which promotes protein expression in certain mouse brain tissues, regulating anxiety-related emotional responses (Yoon et al. 2013). These case studies in neural tissue indicate that for some gene products, the long 3′ UTR specifies translational silencing, while in others it contains sequences that promote active translation, much as we have found in *Drosophila* spermatogenesis. However, only a small selection of the hundreds of genes that display 3′ UTR lengthening due to APA in the nervous system have been assessed for isoform-specific changes in translation. Our results indicating widespread effects of 3′ UTR shortening due to developmentally regulated APA on stage-specific protein expression during spermatogenesis in *Drosophila* strongly suggest that similar global analyses should be conducted on the differentiation of neural progenitors into neurons.

Widespread 3′ UTR shortening due to APA has also been observed during mouse spermatogenesis, although in mammals the major 3′ UTR shortening occurred with the switch from spermatocytes to spermatids (Li et al. 2016). Consistent with our findings, Liu et al. (2007), showed that in mouse spermatogenesis, 3′ UTR shortening (mainly in spermatids) correlated with lower usage of the canonical PAS motif AAUAAA at the proximal cut site (Liu et al. 2007). Extending this, we found for 3′ UTR shortening in *Drosophila* spermatocytes that relatively weak, noncanonical PAS motifs at the proximal

cut site were often paired with strong, canonical PAS motifs for the distal cut site (see Fig. 2 and related text). Indeed, our bioinformatic analyses of sequences upstream of distal cut sites used in spermatogonia revealed an almost threefold increase of the canonical PAS (65.7%) compared with the sequence upstream of the proximal cut sites used in spermatocytes (22.8%) (Fig. 2B). Extending this beyond correlation, we tested the importance of a noncanonical PAS motif upstream of the proximal cut site using reporter constructs in vivo. We found that a single nucleotide change converting a variant, noncanonical PAS into the canonical PAS motif was sufficient to allow cleavage at the proximal site in precursor cells, resulting in a short 3′ UTR isoform instead of the long 3′ UTR isoform normally produced. This demonstrates that the prevalence of noncanonical PAS motifs upstream of the proximal cut site is an important part of the mechanism that allows those proximal cut sites to be skipped in precursor cells so that only the long 3′ UTR isoform is expressed in the early stage cells. In a second potential parallel with 3′ UTR shortening during mammalian spermatogenesis, we found U-rich motifs enriched in the 3′ UTR extensions of the genes that undergo 3′ UTR shortening by APA in *Drosophila* spermatocytes compared with spermatogonia (see Fig. 6E,F). Similarly, Li et al. (2016) showed enrichment for UUUU and related U-rich motifs in the 3′ UTR extensions of genes that demonstrated 3′ UTR shortening by APA in mouse spermatids (Li et al. 2016). This similarity in motif enrichment raises the possibility that underlying mechanisms and consequences may be conserved from *Drosophila* to mammals.

Recently, NMD was shown to play a role in degrading mRNAs with long 3′ UTRs in mouse round spermatids (Bao et al. 2016; Fanourgakis et al. 2016). However, preferential degradation of the long 3′ UTR isoform is not likely to account for the differences in APA that we observed, as our time-course analysis showed that expression of the short 3′ UTR isoform is extremely low in spermatogonia and increases during differentiation (Fig. 1G) for almost all of the ∼500 cases of 3′ UTR shortening that we detected. Thus, the shift from long to short 3′ UTR isoforms in *Drosophila* spermatocytes is not likely due to preferential degradation of long 3′ UTR isoforms. However, we also identified Cnot4 motifs as enriched in 3′ UTR extensions of mRNAs that undergo APA (Fig. 6E,F), consistent with a possible role of NMD in decreasing levels of long 3′ UTR isoforms in differentiating cells.

Our results in the *Drosophila* male germline adult stem cell lineage agree with the findings in HEK293T and five other human cell lines showing that alternative processing of 3′ UTRs broadly influences translation (Floor and Doudna 2016; Fu et al. 2018). Changes in 3′ UTR length may influence regulation by miRNAs, as seen in cancer and activated T lymphocytes, where shortening of transcript 3′ UTRs by APA is thought to allow escape from miRNA targeting (Mayr and Bartel 2009). Also, 3′ UTRs may be bound at specific sequences by numerous RBPs that can influence the stability, localization, and translation of mRNAs, as shown for AU-rich binding proteins known to repress translation (García-Mauriño et al. 2017).

Why might normal cells use such an APA mechanism to regulate changes in protein expression as they advance from one state to the next in a developmental progression? As discussed above, the switch from precursor cell proliferation to the onset of terminal differentiation involves dramatic changes in cellular programs that must be cleanly executed. Developmentally regulated APA may provide a mechanism to rapidly turn off the expression of specific proteins for the prior proliferation program and initiate the expression of proteins involved in the onset of differentiation to facilitate clean and sharp transitions between developmental states. Since APA occurs on nascent transcripts, 3′ UTR shortening that removes sequences that instruct translational repression of the mRNA may facilitate the rapid onset of expression of the encoded protein without having to await chromatin opening, formation of a preinitiation complex, and initiation and elongation of transcripts, as would be required in turning on a new transcription program.

Results of network and gene enrichment analyses were consistent with the idea that an APA-based mechanism to shut off protein expression may aid the transition from mitotic proliferation to the onset of differentiation. Functional network analysis and gene ontology (GO) enrichment analysis using STRING (Szklarczyk et al. 2021) of the 531 genes that undergo APA resulting in shorter 3′ UTRs in differentiating spermatocytes revealed enrichment in the categories of biological process GO term "cell cycle" and cellular component GO term "Polycomb group (PcG) protein complex" (Supplemental Fig. S7A, highlighted in red and blue, respectively). A similar analysis of the 200 genes that undergo 3′ UTR shortening where polysome profiling suggested a switch from active translation of the long 3′ UTR isoform in proliferating spermatogonia (24 h PHS) to a translationally inactive state of the short 3′ UTR isoform in differentiating spermatocytes (48 h PHS) showed enrichment of the biological process GO term "cell cycle process" (Supplemental Fig. S7B, highlighted in red). Enrichment of cell cycle regulators in the set of APA genes predicted to switch from protein expression on in spermatogonia to off in spermatocytes is consistent with previous studies showing that other cell cycle regulatory proteins—PCNA (Insco et al. 2009) and DREF (Angulo et al. 2019)—are abruptly down-regulated after completion of premeiotic S phase and entry into meiotic prophase in the *Drosophila* male germline. PcG components were also enriched among the 531 genes that undergo 3′ UTR shortening by APA, although polysome fractionation results suggested that some may switch from on to off, while others may switch from off to on. In addition to the APA genes noted here, protein expression of the PRC2 components E(z) and Su(z)12 (Chen et al. 2011) have been shown to switch from on to off as spermatogonia differentiate into spermatocytes. Together, the results suggest that there may be widespread changes in protein expression for PcG components during germline differentiation, perhaps reflecting a duty shift between homologs.

An APA-based mechanism to shut off protein expression as precursor cells cease mitosis and initiate

differentiation may be especially important during spermatogenesis, as many cell cycle regulators that could potentially be deleterious early in meiotic prophase are called into action later for spermatocytes to enter and execute the meiotic divisions. In addition, many genes involved in later stages of male germ cell differentiation must be expressed in spermatocytes to endow spermatids with mRNAs that they will translate later. Our 3′-seq analysis of polysome gradient fractions from testes filled with young (48-h PHS) or maturing (72-h PHS) spermatocytes revealed that many mRNA isoforms with shortened 3′ UTRs may become translationally derepressed as spermatocytes mature, moving to migrate with the 80S monosome or polysomal fractions. This dynamic translational regulation following alternative 3′ cleavage may allow differentiating germ cells to repress the expression of specific proteins for a defined but critical period during differentiation onset while still maintaining transcripts for re-expression of the protein at later stages (Fig. 6A–D).

We identified 200 genes subject to stage-specific APA where the long 3′ UTR isoform comigrated with polysomes at 24 h PHS, but the short 3′ UTR isoform expressed at 48 h PHS comigrated with submonosomal fractions, suggesting translational repression. For many of these, the short 3′ UTR isoform was enriched in the gradient fractions containing the 40S small ribosomal subunit at 48 h PHS. Comigration of the short 3′ UTR isoform with the 40S or 60S subribosomal fractions may reflect transcripts accumulating at an intermediate step in translational activation (Sokabe and Fraser 2019). Alternatively, the comigration of many short 3′ UTR mRNA isoforms with the 40S small ribosomal subunit at 48 h PHS that we observed may involve a mechanism where translationally repressed mRNAs are complexed with the 40S ribosomal small subunit, as has been shown in stress granules, regulated by phosphorylation of eIF2 (Panas et al. 2016).

Our combined polysome fractionation and 3′-seq indicated that for half of the ∼500 genes that we identified as subject to 3′ UTR shortening by stage-specific APA, the mRNA isoforms with short 3′ UTRs expressed in young spermatocytes migrated differently in polysome gradient fractions than the mRNA isoforms with long 3′ UTRs expressed in spermatogonia, suggesting changes in translation state. However, changes in protein expression upon APA may be even more widespread. Analysis of protein expression for several genes, including *dco*, *LolaF*, *Chd3*, *numb*, and *CG32066* (Supplemental Fig. S6C–G), showed dramatic up-regulation or down-regulation of protein expression correlating with the timing of 3′ UTR shortening by APA even though the long and short 3′ UTR mRNA isoforms did not show dramatic changes in migration pattern in polysome gradients. It is possible that in some cases translational repression does not result in changes in the polysome profile of the mRNA, perhaps due to cotranslational degradation of mRNAs targeted by microRNAs, as has been shown for 3′ UTR-dependent repression of translation of *hid* by the bantam miRNA and *reaper* by miR-2 in *Drosophila* S2 cells (Tat et al. 2016). Additional studies have shown that regulation of *lin-41* by the *let-7* microRNA or of *lin-14* by the *lin-4* microRNA in *C. elegans* (Olsen and Ambros 1999; Stadler et al. 2012) also occurs without changing the polysome profile of miRNA targeted mRNAs.

Together, our results advance the field considerably by revealing on a global scale what may be the import of developmentally regulated stage-specific 3′ UTR shortening in differentiating cell lineages in vivo. We demonstrate that 3′ UTR shortening due to developmentally regulated APA can lead to widespread changes in the suite of proteins expressed at specific steps in a differentiation sequence. Strikingly, one molecular mechanism—the choice of a more upstream site at which to make the 3′ end cut that terminates nascent transcripts—can turn protein expression either from on to off or from off to on in a gene selective manner presumably controlled by sequences in the longer 3′ UTR expressed in proliferating precursor cells.

Materials and methods

Fly strains and husbandry

Drosophila strains were raised on standard molasses medium at 25°C unless otherwise noted. The following *Drosophila* strains were used: w^{1118} as wild type, bam^{1} (McKearin and Spradling 1990), $bam^{\Delta 86}$ (McKearin and Ohlstein 1995), $bgcn^{1}$ and $bgcn^{63-44}$ (Ohlstein et al. 2000), *bam-Gal4* (Chen and McKearin 2003), aly^{5p} and aly^{2} (White-Cooper et al. 2000), and sa^{1} and sa^{2} (Lin et al. 1996). Tagged FlyFos TransgeneOme (fTRG) (Sarov et al. 2016) stocks were obtained from VDRC.

For the heat shock time course (hsTC), *hs-BamHA/CyO; bam*$^{\Delta 86}$*,e/TM3,e,Sb* males and *bam*^{1}*,e/TM6b,e,Hu* females were crossed on molasses medium at 22°C, adults were removed after 3 d, and ∼9 d after crossing, late stage pupae were shifted for 30 min to a 37°C water bath for heat shock and then incubated for 16, 24, 32, 48, 72, or 96 h at 25°C before collection of *hs-BamHA/+;bam*^{1}*/bam*$^{\Delta 86}$ flies for dissection.

3′-seq data analysis

Reads obtained from sequencing on the Illumina NextSeq 500 platform from libraries created with the QuantSeq 3′ mRNA-seq library preparation kit FWD for Illumina (Lexogen), including oligo dT priming and insert size optimization for shorter read lengths of 50–100 nt, were aligned against the *Drosophila* (dm6) genome using bowtie version 0.12.8 (Langmead et al. 2009) with a value of $e = 5000$ to allow for expected mismatches in the polyA tail not encoded in the genome (Supplemental Fig. S1A). Cleavage sites were defined as the location of the first A in a string of at least 15 contiguous As, requiring that at least three do not match the genome. All cleavage sites reported are supported by at least 20 reads. Minor CSs that were within 50 bp of another cleavage site with a higher read count were discarded. Cleavage sites that did not map to annotated FlyBase 3′ UTRs (r6.36) or within 500 bp downstream from annotated 3′ UTRs were not analyzed in this study. To prevent the association of cleavage sites in 5′ UTRs of neighboring genes with the upstream gene caused by the 500-bp 3′ UTR extension, we did not extend 3′ UTRs into a neighboring gene's 5′ UTR as defined by FlyBase. Cleavage sites were assigned to the closest upstream CDS end as defined by FlyBase.

To identify genes encoding transcript isoforms arising from differential 3′ end cleavage in the hsTC, we identified the main

cleavage site for each transcript in each library, defined as the cleavage site supported by the highest number of reads for each transcript. To call differential 3′ end cleavage of transcripts expressed at different time points, we required the peaks to pass criteria on both biological replicates of a given time point and the distance between the main cleavage sites at different time points to be >100 bp (Supplemental Fig. S1A). Furthermore, we required genes that gave rise to transcripts with different main cleavage sites to have greater than a fourfold difference in expression level between the two isoforms in *bam*$^{-/-}$;*hs-Bam-HA* flies without heat shock versus 16-, 24-, 32-, 48-, or 72-h PHS libraries.

To validate the reproducibility of the 3′-seq protocol in the biological replicates, we plotted the expression of all 3′ cleavage sites expressed in both biological replicates from various time points in the hsTC and *aly* mutant testes (Supplemental Fig. S1C–I). The majority of the data sets have high values for the coefficient of determination R^2 as well as the Pearson correlation coefficient *r*, indicating that the 3′-seq protocol performed on replicate biological tissue from the hsTC testes yielded reproducible results.

MEME motif analysis

Unbiased motif searches on sequences spanning 50 bases upstream of proximal or distal cleavage sites for genes that undergo APA were performed using MEME (Multiple Em for Motif Elucidation) version 5.4.1 (Bailey and Elkan 1994; Bailey et al. 2015), a discriminative motif discovery algorithm. Control sequences were defined as 50 bases upstream of the cleavage site for genes expressed in both *bam*$^{-/-}$;*hs-Bam-HA* flies without heat shock and 48 h PHS that had identical 3′ cleavage site choice for the predominant cleavage site in all biological replicates between *bam* and 48-h PHS 3′-seq libraries. A second-order Markov model was used as the background model.

Additionally, unbiased motif searches on "extension" sequences spanning from the proximal to the distal cleavage sites were performed using MEME for two groups of transcripts that undergo APA: (1) 200 transcripts that change polysome profile from on polysomes to off polysomes and (2) 50 transcripts that change polysome profile from ribosome-free fractions to predominantly on polysomes. Simple enrichment analysis (SEA) in the MEME suite was used to identify miRNA seed sequences in the extension of 3′ UTRs of the 50 transcripts that change polysome profile from ribosome-free fractions to predominantly on polysomes. As before, control sequences were taken from a set of transcripts expressed by both *bam*$^{-/-}$;*hs-Bam-HA* flies without heat shock and 48 h PHS that had identical 3′ cleavage site choice for the predominant cleavage site in all biological replicates between *bam* and 48-h PHS 3′-seq libraries.

Polysome fractionation

For each biological replicate of the polysome fractionation, ~1200 testes (dissected from 600 flies) were used, combining 10 tubes of 120 testes (flash-frozen in liquid nitrogen and stored at −80°C) during the lysis step. Tissue was lysed in buffer containing 25 mM Tris (pH 7.5), 15 mM $MgCl_2$, 150 mM NaCl, 1% Triton X-100, 1 mM DTT, 8% glycerol, and 0.2 mg/mL cycloheximide at 4°C using a 27-gauge 1.5-in syringe to disrupt the tissue, and then the lysate was incubated for 30 min at 4°C while rocking. Ten percent of the supernatant was saved for input, and the remaining supernatant was loaded onto a 50-mL sucrose gradient (10%–40%). Samples were spun down in an ultracentrifuge at 40,000 rpm for 2.5 h at 4°C. Sequential 10-drop fractions were collected from the top using a Brandel gradient fractionator, with absorbance at A260 nm measured continuously during collection to assess RNA concentration. RNA was isolated by acid phenol-chloroform extraction, and fractions were combined based on the absorbance profiles at A260 nm to create six groups: free, 40S, 60S, 80S, two to three ribosomes, and four or more ribosomes. 3′-seq libraries were created using the QuantSeq FWD kit (Lexogen), and reads were mapped and analyzed with the same pipeline outlined above in "3′-Seq Data Analysis" (Supplemental Fig. S1A). Sequencing depth was sufficient for analysis of all biological replicates of 24, 48, and 72 h PHS (Supplemental Fig. S6A–C) except for one replicate of the 72-h PHS 60S polysome fraction, which was discarded due to the low number of reads mapping to gene 3′ UTRs. Read distributions are shown for the orb locus in the polysome profiles from 24, 48, and 72 h PHS in Supplemental Figure S6D–F.

Polysome fractionation analysis

3′-seq reads were normalized to the read count in each library and then normalized across the polysome profile to analyze all transcripts independent of the overall expression. Hierarchical clustering was used to group transcripts with similar polysome profiles. Clusters were then rearranged to reflect the order of the biological process (i.e., the cluster containing transcripts enriched in the free fraction was ordered above the cluster containing transcripts enriched in the 40S fraction, etc.).

Alternative 3′ cleavage analysis using Fly Cell Atlas (FCA) 10X data

Since the FCA 10X reads were always shifted ~200 bases upstream of the CSs identified by 3′-seq (Supplemental Fig. S3A, B), we summed all reads, up to 250 bases upstream of the proximal and distal CSs, to reflect the expression of the proximal and distal CSs in the FCA data set. We then calculated the ratio of proximal: distal CS usage using all reads from nuclei in cluster 25 of Leiden 6.0 (corresponding to spermatogonia) and all reads from nuclei in cluster 35 of Leidein 6.0 (corresponding to early to mid-stage spermatocytes).

Immunofluorescence staining

For whole-mount staining, testes from 0- to 1-d-old males were dissected in 1× phosphate-buffered saline (PBS) and incubated with 4% formaldehyde for 20 min at room temperature. After fixation, the testes were washed once in PBST (PBS with 0.1% Triton X-100) and permeabilized by incubation with PBS with 0.3% Triton X-100 and 0.6% sodium deoxycholate for 30 min at room temperature. After permeabilization, testes were washed once in PBST and blocked for 30 min with PBST containing 3% bovine serum albumin (BSA) and then incubated overnight at 4° C with the desired primary antibodies in PBST with 3% BSA. After overnight incubation in primary antibody, testes were washed three times with PBST, incubated with secondary antibodies conjugated with Alexa fluorophores (Alexa fluor-488, Alexa fluor-568, and Alexa fluor-647 from Molecular Probes) for 2 h at room temperature in the dark while rocking, washed three times in PBST, and mounted on glass slides with mounting medium containing DAPI (VectaShield, Vector Laboratories H-1200).

The sources and dilutions of primary antibodies used were as follows: Vasa (goat; 1:100; Santa Cruz Biotechnology dc-13), Lola-F (mouse; 1:100; DSHB 1F1-1D5), Kumgang (rabbit; 1;400) (Kim et al. 2017), NudE (rabbit; 1:200) (Wainman et al. 2009), Orb (mouse; orb 4H8 and orb 6H4; 1:30; DSHB), and Numb (guinea pig; 1:500) (O'Connor-Giles and Skeath 2003).

Generation of transgenic reporters

The sequence encoding destabilized GFP (Li et al. 1998) flanked with EcoRI and NotI restriction sites was synthesized. Additionally, the sequence encoded in the endogenous *dco* 3′ UTR (total of 1857 nt; "*dco* 3′ UTR WT") flanked with Not1 and Kpn1 restriction sites and a second similar sequence with one base pair change (the 113th T in the *dco* 3′ UTR into an A ["*dco* 3′ UTR can PAS*"]) were synthesized. To create the expression constructs, the pUASTattb vector (Bischof et al. 2007) was digested with EcoRI and KpnI enzymes, gel-purified, and ligated with the sequences encoding the destabilized GFP and one or the other of the *dco* 3′ UTR sequences. These constructs were injected into fly embryos carrying the attp40 site by BestGene, and fly lines that had stably introduced these transgenes into the germline were retained.

Fluorescence microscopy and image analysis

Images of fixed and immunostained testes were taken with either a Leica SP2 or SP8 confocal microscope. Images of native GFP and mRFP fluorescence in unfixed testes were taken with a Leica SP8 microscope. Laser intensity and detector gain for the confocal microscope were adjusted for each experiment to ensure that the signal was in the linear range and not saturated. Once image acquisition settings were determined, the same settings were maintained for the entire set of images to be compared. Immunofluorescence images were processed using ImageJ, with all samples to be compared going through the same processing.

For live imaging of testes expressing fluorescent reporters, newly dissected testes in 1× PBS were immediately placed on a coverslip. To prevent squashing during imaging, two clean coverslips were securely taped on a slide with a gap left in between, and the coverslip with the dissected testes was placed on the slide in the gap with edges overlapping the taped coverslips. Testes were imaged on a Leica SP8 confocal microscope, taking ~40 z-slices with a separation of 2 µm between each, focused on the tip of the testes. Quantification of fluorescence was performed using the program Volocity (PerkinElmer) to sum fluorescence of a 120-µm × 120-µm area positioned to cover the tip of the testes across z-stacks. GFP reporter fluorescence was normalized to His2Av-mRFP fluorescence in each sample.

qRT-PCR and 3′ RACE

RNA was extracted from ~30 pairs of testes by phenol-chloroform separation using Trizol (Life Technologies 15596-026). Total RNA (0.5 µg) was used to make cDNA by using Ready-To-Go You Prime first strand beads (GE Healthcare 27-9264-01) with 0.1 µg of oligo dT or 3′ RACE adapter per reaction (Invitrogen FirstChoice RLM-RACE kit AM1700). After reverse transcription, cDNA was diluted 1/100 in filtered water, and 5–10 µL of diluted cDNA was used per qPCR reaction. To perform qRT-PCR, we mixed 2× SensiFAST SYBR Hi-ROX reagents (Bioline BIO-92020) with cDNA and a final concentration of 125 nM for each primer and measured fluorescence using the 7500 Fast real-time PCR system from Applied Biosystems. The relative abundance of the transcripts was calculated by the $\Delta\Delta Ct$ method. In all qRT-PCR experiments, error bars represent the standard deviation from the mean in three independent biological replicates.

For 3′ RACE, cDNA was generated following manufacturer's instructions (Invitrogen FirstChoice RLM-RACE kit). Briefly, first strand synthesis reaction was carried out with the 3′ RACE adapter (5′-GCGAGCACAGAATTAATACGACTCACTATAGG T_{12}VN-3′) for 1 h at 42°C. The outer PCR reaction was carried out with an outer *lolaF* isoform-specific primer (5′-CGATG ACGAAGACGAGACATT-3′) and the outer primer (5′-GCGAG CACAGAATTAATACGACT-3′) for 35 cycles. One-twentieth of the PCR product was used in the subsequent inner PCR reaction with an inner *lolaF* isoform-specific primer (5′-GATG AACGAGGAGTGGAACAT-3′) as well as the inner primer (5′-CGCGGATCCGAATTAATACGACTCACTATAGG-3′) for 35 cycles.

Protein–protein interaction network and gene ontology (GO) analysis

Protein–protein interaction network analysis was conducted by using STRING (version 11.5) (Szklarczyk et al. 2019, 2021) using a minimum required interaction score of 0.900 (highest confidence) or 0.700 (high confidence). Active interaction sources included in the interaction analysis were (1) experimentally determined interactions, (2) curated pathway databases, and (3) coexpression evidence. GO term enrichments were determined using STRING. As input, the 531 transcripts that undergo APA to produce transcripts with shorter 3′ UTRs in differentiating spermatocytes or 200 transcripts that shorten their 3′ UTR from 24 h PHS to 48 h PHS in the time course and whose translation activity goes from on to off were used.

Competing interest statement

The authors declare no competing interests.

Acknowledgments

We thank Sarah Stern for the UMAP images showing the expression of transcripts encoding RNA binding proteins, indicated by enrichment analysis in testis tissue, based on snRNA-seq data from the Fly Cell Atlas. We thank Dr. Maurizio Gatti for antibodies against NudE, Dr. James Skeath for antibodies against Numb, and Dr. Kristen Johansen and Dr. Jørgen Johansen for antibodies against LolaF. We thank Dr. Maria Barna for suggesting the polysome fractionation approach; Dr. Kathrin Leppek, Dr. Gerald Tiu, and Dr. Shifeng Xue in the Barna laboratory for technical assistance with polysome fractionation; and Dr. Ariel Bazzini for advice on interpreting effects of miRNAs on polysome distribution of their mRNA targets. We acknowledge Dr. Erin Davies and William Joo for their initial observations on alternative *lolaF* isoforms and LolaF protein expression in *Drosophila* testes, and Dr. Erin Sanders for her contributions to the analysis of Numb protein expression in testes during her rotation. We are grateful to the Bloomington *Drosophila* Stock Center and the Vienna *Drosophila* RNAi Center for fly stocks, the Developmental Studies Hybridoma Bank for several antibodies, Cheryl Smith from Arendt Sidow's laboratory for insightful help on library preparation, Reuven Agami for advice on library preparation and 3′-seq analysis, Lars Steinmetz for comments, and members of the Fuller laboratory for helpful discussions and input on the manuscript. C.W.B. was supported by a Stanford Graduate Fellowship and National Institutes of Health (NIH) T32AR007422 (PI: Dr. Paul Khavari). G.H.O. was supported by a Latin American Pew Fellowship, an American Heart Association (AHA) postdoctoral fellowship, and Becas Chile (ANID [Agencia Nacional de Investigación y Desarrollo de Chile]). L.G. was supported by an American-Italian Cancer Foundation Postdoctoral Research fellowship, year 2021–2022. This work was supported by NIH grants R21HD079970, 1R01GM124054, and R35GM136433 and funds from the Reed-Hodgson Professorship in Human Biology to M.T.F. This work was supported in part by award number

1S10OD010580-01A1 from the National Center for Research Resources (NCRR).

Author contributions: C.W.B., G.O.H., and L.G. performed experiments. C.W.B. and G.O.H. analyzed data. C.W.B. performed all 3′-seq and polysome profiling experiments. C.W.B. performed all the bioinformatics analyses. G.R. created an initial pipeline for 3′-seq analysis with supervision from J.B.L. G.O.H. performed 3′ RACE experiments. C.W.B. and G.O.H. designed and analyzed 3′ UTR reports. L.G. performed immunofluorescence experiments. G.O.H. performed functional interaction network analysis. C.W.B. and G.O.H. prepared the figures. C.W.B., G.O.H., and M.T.F. designed the study. C.W.B., G.O.H., and M.T.F. wrote the manuscript, together with feedback from A.G., P.O., and J.B.L. The manuscript was reviewed by all authors.

References

Agarwal V, Lopez-Darwin S, Kelley DR, Shendure J. 2021. The landscape of alternative polyadenylation in single cells of the developing mouse embryo. *Nat Commun* **12:** 5101. doi:10.1038/s41467-021-25388-8

An JJ, Gharami K, Liao GY, Woo NH, Lau AG, Vanevski F, Torre ER, Jones KR, Feng Y, Lu B, et al. 2008. Distinct role of long 3′ UTR BDNF mRNA in spine morphology and synaptic plasticity in hippocampal neurons. *Cell* **134:** 175–187. doi:10.1016/j.cell.2008.05.045

Andreassi C, Luisier R, Crerar H, Darsinou M, Blokzijl-Franke S, Tchern L, Luscombe NM, Cuda G, Gaspari M, Saiardi A, et al. 2021. Cytoplasmic cleavage of IMPA1 3′ UTR is necessary for maintaining axon integrity. *Cell Rep* **34:** 108778. doi:10.1016/j.celrep.2021.108778

Angulo B, Srinivasan S, Bolival BJ, Olivares GH, Spence AC, Fuller MT. 2019. DREF genetically counteracts Mi-2 and Caf1 to regulate adult stem cell maintenance. *PLoS Genet* **15:** e1008187. doi:10.1371/journal.pgen.1008187

Bae B, Miura P. 2020. Emerging roles for 3′ UTRs in neurons. *Int J Mol Sci* **21:** 3413. doi:10.3390/ijms21103413

Bailey TL, Elkan C. 1994. Fitting a mixture model by expectation maximization to discover motifs in biopolymers. *Proc Int Conf Intell Syst Mol Biol* **2:** 28–36.

Bailey TL, Johnson J, Grant CE, Noble WS. 2015. The MEME suite. *Nucleic Acids Res* **43:** W39–W49. doi:10.1093/nar/gkv416

Baker CC, Gim BS, Fuller MT. 2015. Cell type-specific translational repression of cyclin B during meiosis in males. *Development* **142:** 3394–3402. doi:10.1242/dev.122341

Bao J, Vitting-Seerup K, Waage J, Tang C, Ge Y, Porse BT, Yan W. 2016. UPF2-dependent nonsense-mediated mRNA decay pathway is essential for spermatogenesis by selectively eliminating longer 3′UTR transcripts. *PLoS Genet* **12:** e1005863. doi:10.1371/journal.pgen.1005863

Beck AH, Weng Z, Witten DM, Zhu S, Foley JW, Lacroute P, Smith CL, Tibshirani R, van de Rijn M, Sidow A, et al. 2010. 3′-end sequencing for expression quantification (3SEQ) from archival tumor samples. *PLoS One* **5:** e8768. doi:10.1371/journal.pone.0008768

Bischof J, Maeda RK, Hediger M, Karch F, Basler K. 2007. An optimized transgenesis system for *Drosophila* using germ-line-specific φC31 integrases. *Proc Natl Acad Sci* **104:** 3312–3317. doi:10.1073/pnas.0611511104

Chen D, McKearin DM. 2003. A discrete transcriptional silencer in the bam gene determines asymmetric division of the *Drosophila* germline stem cell. *Development* **130:** 1159–1170. doi:10.1242/dev.00325

Chen X, Lu C, Morillo Prado JR, Eun SH, Fuller MT. 2011. Sequential changes at differentiation gene promoters as they become active in a stem cell lineage. *Development* **138:** 2441–2450. doi:10.1242/dev.056572

Cheng LC, Zheng D, Baljinnyam E, Sun F, Ogami K, Yeung PL, Hoque M, Lu CW, Manley JL, Tian B. 2020. Widespread transcript shortening through alternative polyadenylation in secretory cell differentiation. *Nat Commun* **11:** 3182. doi:10.1038/s41467-020-16959-2

Derti A, Garrett-Engele P, Macisaac KD, Stevens RC, Sriram S, Chen R, Rohl CA, Johnson JM, Babak T. 2012. A quantitative atlas of polyadenylation in five mammals. *Genome Res* **22:** 1173–1183. doi:10.1101/gr.132563.111

Di Giammartino DC, Nishida K, Manley JL. 2011. Mechanisms and consequences of alternative polyadenylation. *Mol Cell* **43:** 853–866. doi:10.1016/j.molcel.2011.08.017

Elkon R, Drost J, van Haaften G, Jenal M, Schrier M, Vrielink JA, Agami R. 2012. E2f mediates enhanced alternative polyadenylation in proliferation. *Genome Biol* **13:** R59. doi:10.1186/gb-2012-13-7-r59

Elkon R, Ugalde AP, Agami R. 2013. Alternative cleavage and polyadenylation: extent, regulation and function. *Nat Rev Genet* **14:** 496–506. doi:10.1038/nrg3482

Epstein I, Tushev G, Will TJ, Vlatkovic I, Cajigas IJ, Schuman EM. 2014. Alternative polyadenylation and differential expression of Shank mRNAs in the synaptic neuropil. *Philos Trans R Soc Lond B Biol Sci* **369:** 20130137. doi:10.1098/rstb.2013.0137

Fanourgakis G, Lesche M, Akpinar M, Dahl A, Jessberger R. 2016. Chromatoid body protein TDRD6 supports long 3′ UTR triggered nonsense mediated mRNA decay. *PLoS Genet* **12:** e1005857. doi:10.1371/journal.pgen.1005857

Floor SN, Doudna JA. 2016. Tunable protein synthesis by transcript isoforms in human cells. *Elife* **5:** e10921. doi:10.7554/eLife.10921

Fu Y, Sun Y, Li Y, Li J, Rao X, Chen C, Xu A. 2011. Differential genome-wide profiling of tandem 3′ UTRs among human breast cancer and normal cells by high-throughput sequencing. *Genome Res* **21:** 741–747. doi:10.1101/gr.115295.110

Fu Y, Chen L, Chen C, Ge Y, Kang M, Song Z, Li J, Feng Y, Huo Z, He G, et al. 2018. Crosstalk between alternative polyadenylation and miRNAs in the regulation of protein translational efficiency. *Genome Res* **28:** 1656–1663. doi:10.1101/gr.231506.117

Fuller MT. 1993. Spermatogenesis. In *The development of Drosophila* (ed. Bate M, Martinez-Arias A), pp. 71–147. Cold Spring Harbor Laboratory Press, Cold Spring Harbor, NY.

García-Mauriño SM, Rivero-Rodríguez F, Velázquez-Cruz A, Hernández-Vellisca M, Díaz-Quintana A, De la Rosa MA, Díaz-Moreno I. 2017. RNA binding protein regulation and cross-talk in the control of AU-rich mRNA fate. *Front Mol Biosci* **4:** 71. doi:10.3389/fmolb.2017.00071

Gruber AJ, Zavolan M. 2019. Alternative cleavage and polyadenylation in health and disease. *Nat Rev Genet* **20:** 599–614. doi:10.1038/s41576-019-0145-z

Gruber AR, Martin G, Müller P, Schmidt A, Gruber AJ, Gumienny R, Mittal N, Jayachandran R, Pieters J, Keller W, et al. 2014. Global 3′ UTR shortening has a limited effect on protein abundance in proliferating T cells. *Nat Commun* **5:** 5465. doi:10.1038/ncomms6465

Hilgers V, Perry MW, Hendrix D, Stark A, Levine M, Haley B. 2011. Neural-specific elongation of 3′ UTRs during *Drosophila* development. *Proc Natl Acad Sci* **108:** 15864–15869. doi:10.1073/pnas.1112672108

Insco ML, Leon A, Tam CH, McKearin DM, Fuller MT. 2009. Accumulation of a differentiation regulator specifies transit

amplifying division number in an adult stem cell lineage. *Proc Natl Acad Sci* **106:** 22311–22316. doi:10.1073/pnas.0912454106

Irier HA, Shaw R, Lau A, Feng Y, Dingledine R. 2009. Translational regulation of GluR2 mRNAs in rat hippocampus by alternative 3′ untranslated regions. *J Neurochem* **109:** 584–594. doi:10.1111/j.1471-4159.2009.05992.x

Je G, Guhathakurta S, Yun SP, Ko HS, Kim YS. 2018. A novel extended form of α-synuclein 3′UTR in the human brain. *Mol Brain* **11:** 29. doi:10.1186/s13041-018-0371-x

Ji Z, Tian B. 2009. Reprogramming of 3′ untranslated regions of mRNAs by alternative polyadenylation in generation of pluripotent stem cells from different cell types. *PLoS One* **4:** e8419. doi:10.1371/journal.pone.0008419

Ji Z, Lee JY, Pan Z, Jiang B, Tian B. 2009. Progressive lengthening of 3′ untranslated regions of mRNAs by alternative polyadenylation during mouse embryonic development. *Proc Natl Acad Sci* **106:** 7028–7033. doi:10.1073/pnas.0900028106

Jursnich VA, Fraser SE, Held LI, Ryerse J, Bryant PJ. 1990. Defective gap-junctional communication associated with imaginal disc overgrowth and degeneration caused by mutations of the dco gene in *Drosophila*. *Dev Biol* **140:** 413–429. doi:10.1016/0012-1606(90)90090-6

Kim J, Lu C, Srinivasan S, Awe S, Brehm A, Fuller MT. 2017. Blocking promiscuous activation at cryptic promoters directs cell type-specific gene expression. *Science* **356:** 717–721. doi:10.1126/science.aal3096

Kloss B, Price JL, Saez L, Blau J, Rothenfluh A, Wesley CS, Young MW. 1998. The drosophila clock gene double-time encodes a protein closely related to human casein kinase Iε. *Cell* **94:** 97–107. doi:10.1016/S0092-8674(00)81225-8

Langmead B, Trapnell C, Pop M, Salzberg SL. 2009. Ultrafast and memory-efficient alignment of short DNA sequences to the human genome. *Genome Biol* **10:** R25. doi:10.1186/gb-2009-10-3-r25

Lantz V, Chang JS, Horabin JI, Bopp D, Schedl P. 1994. The *Drosophila* orb RNA-binding protein is required for the formation of the egg chamber and establishment of polarity. *Genes Dev* **8:** 598–613. doi:10.1101/gad.8.5.598

Li X, Zhao X, Fang Y, Jiang X, Duong T, Fan C, Huang CC, Kain SR. 1998. Generation of destabilized green fluorescent protein as a transcription reporter. *J Biol Chem* **273:** 34970–34975. doi:10.1074/jbc.273.52.34970

Li W, Park JY, Zheng D, Hoque M, Yehia G, Tian B. 2016. Alternative cleavage and polyadenylation in spermatogenesis connects chromatin regulation with post-transcriptional control. *BMC Biol* **14:** 6. doi:10.1186/s12915-016-0229-6

Li H, Janssens J, De Waegeneer M, Kolluru SS, Davie K, Gardeux V, Saelens W, David FPA, Brbić M, Spanier K, et al. 2022. Fly cell atlas: a single-nucleus transcriptomic atlas of the adult fruit fly. *Science* **375:** eabk2432. doi:10.1126/science.abk2432

Lianoglou S, Garg V, Yang JL, Leslie CS, Mayr C. 2013. Ubiquitously transcribed genes use alternative polyadenylation to achieve tissue-specific expression. *Genes Dev* **27:** 2380–2396. doi:10.1101/gad.229328.113

Lin TY, Viswanathan S, Wood C, Wilson PG, Wolf N, Fuller MT. 1996. Coordinate developmental control of the meiotic cell cycle and spermatid differentiation in *Drosophila* males. *Development* **122:** 1331–1341. doi:10.1242/dev.122.4.1331

Liu D, Brockman JM, Dass B, Hutchins LN, Singh P, McCarrey JR, MacDonald CC, Graber JH. 2007. Systematic variation in mRNA 3′-processing signals during mouse spermatogenesis. *Nucleic Acids Res* **35:** 234–246. doi:10.1093/nar/gkl919

Lutz CS, Moreira A. 2011. Alternative mRNA polyadenylation in eukaryotes: an effective regulator of gene expression. *Wiley Interdiscip Rev RNA* **2:** 22–31. doi:10.1002/wrna.47

MacDonald CC, Wilusz J, Shenk T. 1994. The 64-kilodalton subunit of the CstF polyadenylation factor binds to pre-mRNAs downstream of the cleavage site and influences cleavage site location. *Mol Cell Biol* **14:** 6647–6654.

Masamha CP, Xia Z, Yang J, Albrecht TR, Li M, Shyu AB, Li W, Wagner EJ. 2014. CFIm25 links alternative polyadenylation to glioblastoma tumour suppression. *Nature* **510:** 412–416. doi:10.1038/nature13261

Mayr C, Bartel DP. 2009. Widespread shortening of 3′UTRs by alternative cleavage and polyadenylation activates oncogenes in cancer cells. *Cell* **138:** 673–684. doi:10.1016/j.cell.2009.06.016

McKearin D, Ohlstein B. 1995. A role for the *Drosophila* bag-of-marbles protein in the differentiation of cystoblasts from germline stem cells. *Development* **121:** 2937–2947. doi:10.1242/dev.121.9.2937

McKearin DM, Spradling AC. 1990. bag-of-marbles: a *Drosophila* gene required to initiate both male and female gametogenesis. *Genes Dev* **4:** 2242–2251. doi:10.1101/gad.4.12b.2242

Miura P, Shenker S, Andreu-Agullo C, Westholm JO, Lai EC. 2013. Widespread and extensive lengthening of 3′ UTRs in the mammalian brain. *Genome Res* **23:** 812–825. doi:10.1101/gr.146886.112

Mohanan NK, Shaji F, Koshre GR, Laishram RS. 2021. Alternative polyadenylation: an enigma of transcript length variation in health and disease. *Wiley Interdiscip Rev RNA* **13:** e1692. doi:10.1002/wrna.1692

Morris AR, Bos A, Diosdado B, Rooijers K, Elkon R, Bolijn AS, Carvalho B, Meijer GA, Agami R. 2012. Alternative cleavage and polyadenylation during colorectal cancer development. *Clin Cancer Res* **18:** 5256–5266. doi:10.1158/1078-0432.CCR-12-0543

Mueller AA, Cheung TH, Rando TA. 2013. All's well that ends well: alternative polyadenylation and its implications for stem cell biology. *Curr Opin Cell Biol* **25:** 222–232. doi:10.1016/j.ceb.2012.12.008

O'Connor-Giles KM, Skeath JB. 2003. Numb inhibits membrane localization of sanpodo, a four-pass transmembrane protein, to promote asymmetric divisions in *Drosophila*. *Dev Cell* **5:** 231–243. doi:10.1016/S1534-5807(03)00226-0

Ohlstein B, Lavoie CA, Vef O, Gateff E, McKearin DM. 2000. The *Drosophila* cystoblast differentiation factor, *benign gonial cell neoplasm*, is related to DExH-box proteins and interacts genetically with *bag-of-marbles*. *Genetics* **155:** 1809–1819. doi:10.1093/genetics/155.4.1809

Olsen PH, Ambros V. 1999. The lin-4 regulatory RNA controls developmental timing in *Caenorhabditis elegans* by blocking LIN-14 protein synthesis after the initiation of translation. *Dev Biol* **216:** 671–680. doi:10.1006/dbio.1999.9523

Panas MD, Ivanov P, Anderson P. 2016. Mechanistic insights into mammalian stress granule dynamics. *J Cell Biol* **215:** 313–323. doi:10.1083/jcb.201609081

Pereira-Castro I, Moreira A. 2021. On the function and relevance of alternative 3′-UTRs in gene expression regulation. *Wiley Interdiscip Rev RNA* **12:** e1653. doi:10.1002/wrna.1653

Proudfoot NJ, Brownlee GG. 1976. 3′ non-coding region sequences in eukaryotic messenger RNA. *Nature* **263:** 211–214. doi:10.1038/263211a0

Retelska D, Iseli C, Bucher P, Jongeneel CV, Naef F. 2006. Similarities and differences of polyadenylation signals in human and fly. *BMC Genomics* **7:** 176. doi:10.1186/1471-2164-7-176

Sandberg R, Neilson JR, Sarma A, Sharp PA, Burge CB. 2008. Proliferating cells express mRNAs with shortened 3′ untranslated

regions and fewer microRNA target sites. *Science* **320:** 1643–1647. doi:10.1126/science.1155390

Sarov M, Barz C, Jambor H, Hein MY, Schmied C, Suchold D, Stender B, Janosch S, K J VV, Krishnan RT, et al. 2016. A genome-wide resource for the analysis of protein localisation in *Drosophila*. *Elife* **5:** e12068. doi:10.7554/eLife.12068

Sasaki S, Shionoya A, Ishida M, Gambello MJ, Yingling J, Wynshaw-Boris A, Hirotsune S. 2000. A LIS1/NUDEL/cytoplasmic dynein heavy chain complex in the developing and adult nervous system. *Neuron* **28:** 681–696. doi:10.1016/S0896-6273(00)00146-X

Shi Y. 2012. Alternative polyadenylation: new insights from global analyses. *RNA* **18:** 2105–2117. doi:10.1261/rna.035899.112

Shigeoka T, Jung H, Jung J, Turner-Bridger B, Ohk J, Lin JQ, Amieux PS, Holt CE. 2016. Dynamic axonal translation in developing and mature visual circuits. *Cell* **166:** 181–192. doi:10.1016/j.cell.2016.05.029

Skora AD, Spradling AC. 2010. Epigenetic stability increases extensively during *Drosophila* follicle stem cell differentiation. *Proc Natl Acad Sci* **107:** 7389–7394. doi:10.1073/pnas.1003180107

Smibert P, Miura P, Westholm JO, Shenker S, May G, Duff MO, Zhang D, Eads BD, Carlson J, Brown JB, et al. 2012. Global patterns of tissue-specific alternative polyadenylation in *Drosophila*. *Cell Rep* **1:** 277–289. doi:10.1016/j.celrep.2012.01.001

Sokabe M, Fraser CS. 2019. Toward a kinetic understanding of eukaryotic translation. *Cold Spring Harb Perspect Biol* **11:** a032706. doi:10.1101/cshperspect.a032706

Sommerkamp P, Cabezas-Wallscheid N, Trumpp A. 2021. Alternative polyadenylation in stem cell self-renewal and differentiation. *Trends Mol Med* **27:** 660–672. doi:10.1016/j.molmed.2021.04.006

Spies N, Burge CB, Bartel DP. 2013. 3′ UTR-isoform choice has limited influence on the stability and translational efficiency of most mRNAs in mouse fibroblasts. *Genome Res* **23:** 2078–2090. doi:10.1101/gr.156919.113

Spillantini MG, Schmidt ML, Lee VM, Trojanowski JQ, Jakes R, Goedert M. 1997. α-Synuclein in Lewy bodies. *Nature* **388:** 839–840. doi:10.1038/42166

Stadler M, Artiles K, Pak J, Fire A. 2012. Contributions of mRNA abundance, ribosome loading, and post- or peri-translational effects to temporal repression of *C. elegans* heterochronic miRNA targets. *Genome Res* **22:** 2418–2426. doi:10.1101/gr.136515.111

Szklarczyk D, Gable AL, Lyon D, Junge A, Wyder S, Huerta-Cepas J, Simonovic M, Doncheva NT, Morris JH, Bork P, et al. 2019. STRING v11: protein–protein association networks with increased coverage, supporting functional discovery in genome-wide experimental datasets. *Nucleic Acids Res* **47:** D607–D613. doi:10.1093/nar/gky1131

Szklarczyk D, Gable AL, Nastou KC, Lyon D, Kirsch R, Pyysalo S, Doncheva NT, Legeay M, Fang T, Bork P, et al. 2021. The STRING database in 2021: customizable protein–protein networks, and functional characterization of user-uploaded gene/measurement sets. *Nucleic Acids Res* **49:** D605–D612. doi:10.1093/nar/gkaa1074

Taliaferro JM, Vidaki M, Oliveira R, Olson S, Zhan L, Saxena T, Wang ET, Graveley BR, Gertler FB, Swanson MS, et al. 2016. Distal alternative last exons localize mRNAs to neural projections. *Mol Cell* **61:** 821–833. doi:10.1016/j.molcel.2016.01.020

Tat TT, Maroney PA, Chamnongpol S, Coller J, Nilsen TW. 2016. Cotranslational microRNA mediated messenger RNA destabilization. *Elife* **5:** e12880. doi:10.7554/eLife.12880

Terenzio M, Koley S, Samra N, Rishal I, Zhao Q, Sahoo PK, Urisman A, Marvaldi L, Oses-Prieto JA, Forester C, et al. 2018. Locally translated mTOR controls axonal local translation in nerve injury. *Science* **359:** 1416–1421. doi:10.1126/science.aan1053

Tian B, Hu J, Zhang H, Lutz CS. 2005. A large-scale analysis of mRNA polyadenylation of human and mouse genes. *Nucleic Acids Res* **33:** 201–212. doi:10.1093/nar/gki158

Tushev G, Glock C, Heumüller M, Biever A, Jovanovic M, Schuman EM. 2018. Alternative 3′ UTRs modify the localization, regulatory potential, stability, and plasticity of mRNAs in neuronal compartments. *Neuron* **98:** 495–511.e6. doi:10.1016/j.neuron.2018.03.030

Ulitsky I, Shkumatava A, Jan CH, Subtelny AO, Koppstein D, Bell GW, Sive H, Bartel DP. 2012. Extensive alternative polyadenylation during zebrafish development. *Genome Res* **22:** 2054–2066. doi:10.1101/gr.139733.112

Vicario A, Colliva A, Ratti A, Davidovic L, Baj G, Gricman Ł, Colombrita C, Pallavicini A, Jones KR, Bardoni B, et al. 2015. Dendritic targeting of short and long 3′ UTR BDNF mRNA is regulated by BDNF or NT-3 and distinct sets of RNA-binding proteins. *Front Mol Neurosci* **8:** 62. doi:10.3389/fnmol.2015.00062

Wainman A, Creque J, Williams B, Williams EV, Bonaccorsi S, Gatti M, Goldberg ML. 2009. Roles of the *Drosophila* NudE protein in kinetochore function and centrosome migration. *J Cell Sci* **122:** 1747–1758. doi:10.1242/jcs.041798

White-Cooper H, Schäfer MA, Alphey LS, Fuller MT. 1998. Transcriptional and post-transcriptional control mechanisms coordinate the onset of spermatid differentiation with meiosis I in *Drosophila*. *Development* **125:** 125–134. doi:10.1242/dev.125.1.125

White-Cooper H, Leroy D, MacQueen A, Fuller MT. 2000. Transcription of meiotic cell cycle and terminal differentiation genes depends on a conserved chromatin associated protein, whose nuclear localisation is regulated. *Development* **127:** 5463–5473. doi:10.1242/dev.127.24.5463

Xia Z, Donehower LA, Cooper TA, Neilson JR, Wheeler DA, Wagner EJ, Li W. 2014. Dynamic analyses of alternative polyadenylation from RNA-seq reveal a 3′-UTR landscape across seven tumour types. *Nat Commun* **5:** 5274. doi:10.1038/ncomms6274

Xu C, Zhang J. 2020. A different perspective on alternative cleavage and polyadenylation. *Nat Rev Genet* **21:** 63. doi:10.1038/s41576-019-0198-z

Yoon Y, McKenna MC, Rollins DA, Song M, Nuriel T, Gross SS, Xu G, Glatt CE. 2013. Anxiety-associated alternative polyadenylation of the serotonin transporter mRNA confers translational regulation by hnRNPK. *Proc Natl Acad Sci* **110:** 11624–11629. doi:10.1073/pnas.1301485110

Zhang W, Wang Y, Long J, Girton J, Johansen J, Johansen KM. 2003. A developmentally regulated splice variant from the complex lola locus encoding multiple different zinc finger domain proteins interacts with the chromosomal kinase JIL-1. *J Biol Chem* **278:** 11696–11704. doi:10.1074/jbc.M213269200

Zhang H, Lee JY, Tian B. 2005. Biased alternative polyadenylation in human tissues. *Genome Biol* **6:** R100. doi:10.1186/gb-2005-6-12-r100

Developmentally regulated alternate 3′ end cleavage of nascent transcripts controls dynamic changes in protein expression in an adult stem cell lineage

Cameron W. Berry, Gonzalo H. Olivares, Lorenzo Gallicchio, et al.

Genes Dev. 2022, **36:** originally published online September 29, 2022
Access the most recent version at doi:10.1101/gad.349689.122